University of Alberta Library
0 1620 3448568 8

GAS-LIQUID FLOW IN VERTICAL PIPES

B. A. RADFORD

For Reference

NOT TO BE TAKEN FROM THIS ROOM

Ex libris
Universitatis
Albertaensis

UNIVERSITY
OF
ALBERTA
PRINTING DEPT.

Digitized by the Internet Archive
in 2018 with funding from
University of Alberta Libraries

https://archive.org/details/gasliquidflowinv00radf

GAS-LIQUID FLOW
in
VERTICAL PIPES

A Preliminary Investigation

UNIVERSITY OF ALBERTA

SCHOOL OF GRADUATE STUDIES

This is to certify that the undersigned have read and recommended to the Committee on Graduate Studies for acceptance, a thesis submitted by B. A. Radford, B.Sc. "1948", entitled:

GAS-LIQUID FLOW
in
VERTICAL PIPES

A Preliminary Investigation

THESIS

GAS-LIQUID FLOW
in
VERTICAL PIPES
A Preliminary Investigation

Submitted as the Partial Fulfillment
of the
Requirements for the Degree of
Master of Science
in
Chemical Engineering

by
B. A. Radford

Under the direction of
Dr. G. W. Govier

University of Alberta
Edmonton, Alberta.

November, 1949

Bruce A. Radford
Signature of Author

UNIVERSITY LIBRARY
UNIVERSITY OF ALBERTA

Thesis
1950
#41

THE PROBLEM

The problem undertaken was a preliminary investigation into the mechanism and pressure drop--rate of flow relationship for gas-liquid mixtures flowing in vertical pipes. The two principal objectives of the present study are:

1. To make visual observations of the flow mechanisms over a wide range of conditions.
2. To obtain experimental pressure drop data under varying conditions and to make a preliminary interpretation of these data.

SUMMARY

Pressure drop versus rate of flow data have been determined for air-water mixtures flowing through a vertical, 22.88-ft. section of smooth butyrate tubing having an inside diameter of 1.049 inches. For seven constant water rates varying from .000400 ft^3/sec. to .00500 ft^3/sec., the air rates were varied from zero to approximately one ft^3/sec. The pressure drops, the air-water discharge ratios and the air-water ratios in the test section were measured. Visual observations of the flow pattern were made.

This preliminary analysis showed that as the air rate increased from zero the measured pressure drop passed through a first minimum point, a maximum point, a second minimum point and then increased smoothly for each constant water rate. Closely related to the change in pressure was a transition in the flow pattern from "slug" flow, to "froth" flow, to "film" flow and, finally, to "mist" flow.

The first minimum, the result of a rapid decrease in hydrostatic head, was characterized by "slug" flow. The pressure increase from the first minimum point to the maximum point was accompanied by a transition to pulsating, frothy flow. The rapid increase in the relative velocity of the air to the water indicated that "slippage" due to water holdup was mainly responsible for the increase in the pressure gradient. As the air rate was further increased, the pulsating "froth" flow gradually gave way to "film" flow and the measured pressure drop decreased to a second minimum point. During this decrease in pressure drop there was a decrease in the relative velocity of the air to the water. At higher rates the film disappeared and the vertical section was filled with rapidly flowing mist. The measured pressure

drop for the "mist" flow increased smoothly with increased air rates, and appeared to be due mainly to wall friction.

Results indicated that the "film" minimum point and the "froth" maximum point disappear at some higher water rate. The maximum and minimum pressure drop conditions for the various constant water rates occurred at similar air rates. This indicated that the flow pattern depends mainly on the air rate, and suggested that a modified Reynolds number based on the air rate might be used for further interpretive work.

ACKNOWLEDGEMENT

The author wishes to express appreciation to Dr. G. W. Govier under whose supervision this project was carried out and whose criticism and assistance have contributed greatly to the investigation.

Acknowledgement is also made to Dr. D. B. Robinson and Mr. A. L. Scott for their interest and guidance.

The author is indebted to

The Canadian Industries Limited for granting him a fellowship which enabled him to carry out the project, and to the Department of Chemical Engineering of the University of Alberta for the equipment and supplies used in the investigation.

Appreciation is also expressed to Mr. H. L. Bertrand and Mr. C. E. Newman who helped with the construction of the equipment and to Mr. W. Wanat for his assistance in the calibration of the critical flow prover.

TABLE OF CONTENTS

Statement of the Problem

Summary

Acknowledgement

Table of Tables

Table of Figures

		Page
I	Introduction	1
II	Literature Review and Theory	2
III	Experimental Equipment	14
IV	Experimental Procedures	27
V	Experimental Data	29
VI	Calculated Results	35
VII	Interpretation and Correlation of Results	38
VIII	Conclusions	58

APPENDICES

A - Calibrations	60
B - Experimental Data	65
C - Calculated Results	76

Nomenclature

Bibliography

TABLE OF TABLES

Table		Page
I	Calibration of Water Orifice Plate	60
II	Air Orifice Calibration Data	62
III	Air Orifice Calibration Results	63
IV	Calibration of Brooks Rotameter	64
V	Supplementary Data	65
VI	Water Flow Data -- Series A	66
VII	Water Flow Data -- Series B	67
VIII	Water Flow Data -- Series C	68
IX	Air-Water Data -- Constant Water Rate-- 4.15 lbs/sec.ft^2	69
X	Air-Water Data -- Constant Water Rate-- 5.70 lbs/sec.ft^2	70
XI	Air-Water Data -- Constant Water Rate-- 8.10 lbs/sec.ft^2	71
XII	Air-Water Data -- Constant Water Rate-- 12.46 lbs/sec.ft^2	72
XIII	Air-Water Data -- Constant Water Rate-- 17.75 lbs/sec.ft^2	73
XIV	Air-Water Data -- Constant Water Rate-- 25.1 lbs/sec.ft^2	74
XV	Air-Water Data -- Constant Water Rate-- 51.8 lbs/sec.ft^2	75
XVI	Water Flow Results -- Series A	76
XVII	Water Flow Results -- Series B	77
XVIII	Water Flow Results -- Series C	78
XIX	Air-Water Calculated Results -- Constant Water Rate-- 4.15 lbs/sec.ft^2	79
XX	Air-Water Calculated Results -- Constant Water Rate-- 5.70 lbs/sec.ft^2	80

TABLE OF TABLES

Table		Page
XXI	Air-Water Calculated Results -- Constant Water Rate-- 8.10 lbs/sec.ft^2	81
XXII	Air-Water Calculated Results -- Constant Water Rate-- 12.46 lbs/sec.ft^2	82
XXIII	Air-Water Calculated Results -- Constant Water Rate-- 17.75 lbs/sec.ft^2	83
XXIV	Air-Water Calculated Results -- Constant Water Rate-- 25.1 lbs/sec.ft^2	84
XXV	Air-Water Calculated Results -- Constant Water Rate-- 51.8 lbs/sec.ft^2	85
XXVI	Variation of Holdup with Air-Water Discharge Ratio	86
XXVII	Variation of Pressure Drops and Air-Water Discharge Ratios of the Maximum and Minimum Points with Water Rates	87
XXVIII	Variation of the Air-Rates of the Maximum and Minimum Points with Water Rates	88

TABLE OF FIGURES

Figure		Page No.
1	Flow Circuit	15
2	Pressure Connections	17
3	Panel Board and Air Measuring Section	18
4	Mixing Sections and Bottom of Vertical Flow Sections	19
5	Upper Vertical Flow Section	21
6	Plastic Pressure Tap and Connection between the Plastic Tubing and the Iron Pipe	22
7	Panel Board	24
8	Mercury Traps (Rear of Panel Board)	26
9	Critical Flow Prover	30
10	Water Orifice Calibration Data	31
11	Water Test Data	39
12	Effect of the Discharge Air-Water Ratio on Pressure Drop Showing the Hydrostatic Head Equivalent of the Mixture in the Test Section	40
13	Effect of the Discharge Air-Water Ratio on the Air-Water Ratio in the Test Section	43
14	Effect of the Discharge Air-Water Ratio on the Ratio of the Discharge to the Test Section Air-Water Ratio	45
15	Effect of the Discharge Air-Water Ratio on the Pressure Drop Showing the Hydrostatic Head Equivalent of the Discharge Mixture (Constant Water Rate--4.15 lbs/ft.^{2}sec.)	47
16	Effect of the Discharge Air-Water Ratio on the Pressure Drop Showing the Hydrostatic Head Equivalent of the Discharge Mixture (Constant Water Rate--5.70 lbs/ft.^{2}sec.)	48
17	Effect of the Discharge Air-Water Ratio on the Pressure Drop Showing the Hydrostatic Head Equivalent of the Discharge Mixture (Constant Water Rate--8.10 lbs/ft.^{2}sec.)	49
18	Effect of the Discharge Air-Water Ratio on the Pressure Drop Showing the Hydrostatic Head Equivalent of the Discharge Mixture (Constant Water Rate--12.46 lbs/ft.^{2}sec.)	50

TABLE OF FIGURES

Figure		Page No.
19	Effect of the Discharge Air-Water Ratio on the Pressure Drop Showing the Hydrostatic Head Equivalent of the Discharge Mixture (Constant Water Rate--17.75 lbs/ft.^{2}sec.)	51
20	Effect of the Discharge Air-Water Ratio on the Pressure Drop Showing the Hydrostatic Head Equivalent of the Discharge Mixture (Constant Water Rate--25.1 lbs/ft.^{2}sec.)	52
21	Effect of the Discharge Air-Water Ratio on the Pressure Drop Showing the Hydrostatic Head Equivalent of the Discharge Mixture (Constant Water Rate--51.8 lbs/ft.^{2}sec.)	53
22	Effect of the Water Rate on the Maximum and Minimum Pressure Drops	55
23	Effect of Water Rate on the Air-Water Ratios Corresponding With the Maximum and Minimum Pressure Drops	56

I

INTRODUCTION

A growing need exists for a clearer understanding of the mechanism and laws governing the flow of gas-liquid mixtures in vertical pipes. An outstanding example is in the flow of gas-oil mixtures through the "production tubing" of oil wells operated either by gas lift or natural flow. Here the accurate design of a tubing installation for given conditions requires quantitative data of the pressure loss suffered by the oil-gas mixture during its passage through the well tubing to the surface. Due to the scarcity of information the problem is usually approached by "cut-and-try" methods which may well result in tubing larger or smaller than that which would permit the most effective use of the gas lifting the oil.

In the case of the operation of the air lift pump there is a scarcity of workable equations based on a theoretical analysis. Also, the accurate designing of tubing for two-phase flow in tubes such as in long tube vertical evaporators and water tube boilers requires a knowledge of the pressure drop in the tube.

While some work has been done along these lines, no satisfactory solution to the problem is reported in the literature.

II

LITERATURE REVIEW AND THEORY

The pattern of the vertical flow of gas-liquid mixtures varies widely but basically it is either one or a combination of the following four types.

1. A dispersed phase of gas bubbles throughout the liquid.
2. A dispersed phase of liquid droplets throughout the gas.
3. Alternate slugs of gas and liquid.
4. A core of gas flowing through an annular ring of liquid.

A visual study by Cromer(1) showed a gradual change in the type of flow as the gas-liquid ratio was increased. Cromer, working with an air-water system, found that at gas-liquid volume discharge ratios below unity, the flowing mixture consisted of a dispersed phase of bubbles throughout the liquid. When the gas-liquid ratio was increased to about three these bubbles merged into a series of bullet-shaped gas slugs. The gas slugs were separated from each other by "pistons" of liquid. Around the gas slugs annular rings of liquid flowed downwards. Cromer also observed that as the mixture rose, a uniform merging of the gas slugs occurred. The flow pattern was not changed significantly by increasing the gas-liquid ratio to eight although the "pistons" between the gas slugs became increasingly "frothy"--that is, small gas bubbles were dispersed in the liquid.

Cromer dealt mainly with gas liquid ratios below ten. He mentioned, however, that at higher ratios he observed that the flow pattern consisted of a central core of saturated gas flowing through an annular ring of liquid.

The vertical flow of gas-liquid mixtures appears always to be characterized by "liquid holdup"--that is, the discharge ratio of the gas-liquid mixture exceeds the ratio in the tube. The explanation for this phenomenon is the difference in the velocity of the gas relative to the liquid, that is, the liquid moves more slowly through the tube than does the gas. Versuluys(7) showed that for vertically flowing gas-liquid mixtures the ratio of gas to liquid in the tube is dependent not only on the velocity of the gas relative to the liquid, but also on the gas-liquid discharge ratio.

Observations of Cromer(1) and Versuluys(7) demonstrate that, in the case of vertical flow of gas-liquid mixtures, the flow pattern, the flowing gas-liquid ratio and the velocity of the gas relative to the liquid are all interdependent.

In the case of a single phase fluid in a vertical pipe upward flow occurs when the difference between the pressures at the top and bottom of the pipe exceeds the hydrostatic head of fluid. It is reasonable to assume this is also true for gas-liquid mixtures in vertical pipes. Therefore, since the hydrostatic head appears related directly to liquid holdup, the latter is extremely important. The relationship between holdup and the overall pressure drop for gas-liquid flow in vertical pipes was investigated by Moore and Wilde in 1931(4). These workers assumed that the pressure differential could be considered in terms of several components, that is:

$$(P_B - P_T) = -\Delta P = -\Delta P_{LH} - \Delta P_F - \Delta P_{uL} - \Delta P_{uG} - \Delta P_{GH} \quad (1)$$

where, P_T = pressure at the top of the section.

P_B = pressure at the bottom of the section.

$-\Delta P_F$ = pressure drop due to frictional effects.

ΔP_{LH} = pressure drop due to hydrostatic head of liquid.
ΔP_{GH} = pressure drop due to hydrostatic head of gas.
ΔP_{uL} = pressure drop due to the velocity head of liquid.
ΔP_{uG} = pressure drop due to the velocity head of gas.

Since $-\Delta P_{uG}$, $-\Delta P_{uL}$ and $-\Delta P_{GH}$ are negligible, Moore and Wilde assumed that for practical purposes

$$-\Delta P = -\Delta P_F - \Delta P_{LH} \qquad (2)$$

Moore and Wilde's approach was to develop a method whereby, knowing the gas-liquid discharge ratio and the rate of discharge, it would be possible to solve for the two-pressure gradient terms in equation (2). They developed equations whereby the fraction volume of liquid in the pipe could be calculated when the discharge ratio and rate were known. Moore and Wilde believed that knowing the fraction of liquid in the pipe it was possible to calculate the liquid hydrostatic head using the following equation:

$$-\Delta P_{LH} = y \, \rho_L \, H \qquad (3)$$

where, y = volume fraction of pipe occupied by the liquid
ρ_L = density of the liquid
H = height of the vertical section

However, it appears extremely doubtful if the use of this equation is valid for the various flow patterns encountered in the vertical flow of gas-liquid mixtures. This can be best illustrated by annular flow, that is, a core of gas flowing through the centre, surrounded by an annular ring of liquid moving upwards at a slower rate.

[illegible]

[illegible]

$$[illegible]$$

[illegible]

$$[illegible]$$

[illegible]

[illegible]

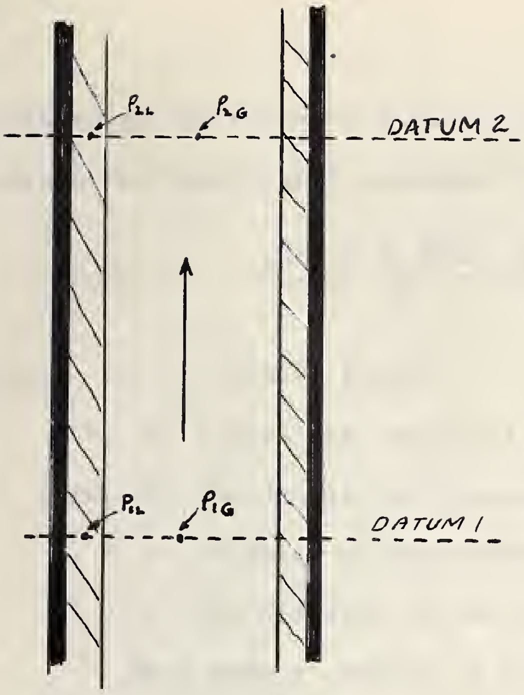

At datum (1) all points in the datum are necessarily the same pressure, so $P_{1L} = P_{1G}$. By the same reasoning at datum (2) $P_{2L} = P_{2G}$. Therefore the total pressure drop between datum (1) and datum (2) is:

$P_{1G} - P_{2G}$ = hydrostatic head of gas + frictional effects = $P_{1L} - P_{2L}$

In the case illustrated no account is taken of the hydrostatic head of the liquid in the pipe. Regarding the annular ring of liquid it seems logical that the weight of the liquid plus the wall friction are opposed by the tractive forces at the gas liquid interface. Therefore it appears that the use of the equation $-\Delta P_{LH} = y \rho_L H$ is not valid and apparently the hydrostatic head is related not only to the fraction of liquid in the tube but also to the pattern of flow. It also might be mentioned that Moore and Wilde found that the equation they experimentally developed for calculating the fraction of liquid in the pipes was not valid in oil wells.

Since the remainder of their work was dependent on the value of $-\Delta P_{LH}$ it appears doubtful if the results are valid. However Moore and Wilde were one of the first who recognized and tried to account for the effects of liquid holdup.

Uren et al.(6) approached the problem of gas-liquid flow in vertical pipes in a different manner. Having considered the variables

influencing the pressure loss they assumed the Fanning equation to include the significant variables involved.

$$- \Delta P = \frac{.323\ f\ N_e\ \rho\ av.\ V^2}{D} \qquad (4)$$

where, f = friction factor

N_e = equivalent length of the section

ρ av. = the density of the mixture

V = velocity of the mixture

D = the diameter of the pipe

They made a series of experimental runs, and for each run measured ΔP and calculated V and ρ av. Then using equation (4) they solved for f. Unfortunately they neglected to mention how the velocity of the mixture was calculated, or whether the pressure drop included the hydrostatic head effect.

In calculating the viscosity of the mixture they used Poiseuille's equation

$$- \Delta P = \frac{.000668\ \mu\ N_e\ V}{D^2} \qquad (5)$$

where, μ = the viscosity of the mixture

Uren et al. assumed that this equation was applicable over the entire range of turbulent and viscous flow. In making this incorrect assumption they arbitrarily made $f = \frac{.00207}{Re.}$

where the Reynolds number, Re. $= \frac{D\ V\ \rho\ av.}{\mu}$ (6)

Since the viscosity for each test was calculated using equation (5) a log-log plot of the friction factor versus the Reynolds number naturally showed a straight-line relationship.

While the paper of Uren et al. does not present a solution to the problem of gas-liquid flow in vertical pipes, it is valuable in that it suggests a method of approach in reaching a workable solution to this important engineering problem.

Gosiline(3) investigated the tractive force at the gas-liquid interface for annular flow of gas-liquid mixtures in vertical pipes. Using theoretical equations and measuring the gas core flow rate, he made a plot of the coefficient of drag versus the velocity of the gas. The plot showed the coefficient decreased with higher gas core velocities. At low gas velocities viscosity was important, that is, liquids having a larger viscosity had a larger drag coefficient. However, at gas core velocities above 90 ft/sec. the influence of viscosity was negligible and the drag coefficient was small and fairly constant.

Gosiline's work was restricted to annular flow of gas-liquid mixtures, and was applicable only to the liquids and pipe diameters he worked with. However, it provides a much clearer understanding of the variables affecting the tractive force at the gas-liquid interface.

The approaches used by Gosiline, Moore, Uren et al. towards the problem of gas-liquid flow in vertical pipes resulted in a better understanding of the difficulties involved but failed to provide a workable solution.

The relationships between the liquid holdup, the hydrostatic head, the flow pattern and the gas-liquid discharge ratio are still very obscure. Without a better knowledge of the holdup in the tube it is not possible to calculate the average velocity, the density or viscosity of the mixture in the pipe.

The present work was undertaken as a first step in a program

designed at overcoming some of the difficulties mentioned above. In order to avoid the complexities and uncertainties of a mechanistic study, the powerful general approach of thermodynamics was employed. The thermodynamic analysis may be introduced through its application to the simpler problem of vertical flow of a single phase of fluid in a circular pipe.

Consider any vertical flow system receiving and discharging a single phase fluid at a uniform rate. A total energy balance (first law of thermodynamics) for m pounds of fluid reveals that(2):

$$\Delta U + \frac{\Delta m g X}{\beta} + \frac{\Delta m V^2}{2\alpha\beta} = q - w \qquad (7)$$

where,

ΔU = all the energy of the system exclusive of potential and kinetic energy

m = mass - lbs.

X = position above datum - ft.

q = heat transfer of energy - units

w = all other forms of energy transferred - units

g = local acceleration of gravity ft/sec^2

β = constant of proportionality - $\frac{\text{mass lbs.}}{\text{force lbs.}} \; \frac{\text{ft.}}{\text{sec}^2}$

V = velocity - ft/sec

For fluid flow, essentially,

$$\Delta U = m\int T\,dS + m\int P\,(-dv) + m\int \gamma\, d\sigma \text{, neglecting other IdE terms} \qquad (8)$$

where, T = absolute temperature - $^{\circ}$R

P = pressure - p.s.i., abs.

v = specific volume - ft.^{3}/lb.

γ = surface tension - lbs. force/ft.

σ = surface area of system - ft.^{2}

and $$-w = -w_s - \Delta Pv \qquad (9)$$

where, w_s = shaft work

also $$\Delta Pv = \int v\, dP + \int P\, dv \qquad (10)$$

combining equations (7), (8), (9), and (10)

$$m\int T\, dS + m\int v\, dP + m\int \gamma\, d\sigma + \frac{\Delta\, m\, g\, X}{\beta} + \frac{\Delta\, m\, V^2}{2\alpha\beta} = q - w_s \qquad (11)$$

however, $$\int T\, dS = q + w_f \qquad (12)$$

where, w_f = "friction" energy

therefore,

$$m\int v\, dP + m\int \gamma\, d\sigma + \frac{\Delta\, m\, g\, X}{\beta} + \frac{\Delta\, m\, V^2}{2\alpha\beta} = -w_f - w_s \qquad (13)$$

calling $w_f = \Sigma F$

and $$\Sigma F = m\frac{\Delta P}{\rho} = \frac{2\, f\, V^2\, N_e}{\beta\, D}\, m \qquad (14)$$

where, $$2f = \phi\left(\frac{D\, V\rho}{\mu}, \frac{\Delta}{D}\right) \qquad (15)$$

Then substituting for w_f and eliminating w_s since there is no shaft work:

$$m\int v\, dP + m\int \gamma\, d\sigma + \frac{\Delta\, m\, g\, X}{\beta} + \frac{\Delta\, m\, V^2}{2\alpha\beta} = -\frac{2f\, V^2\, N_e}{\beta\, D}\, m \qquad (16)$$

where, N_e = equivalent length of the section - ft.

f = friction factor

ρ = density fluid - lbs./ft.^{3}

μ = viscosity of the fluid

D = diameter of the pipe

$\frac{\Delta}{D}$ = roughness factor

Changing equation to the differential form gives:

$$m\,v\,dP + m\gamma\,d\sigma + \frac{m\,g\,dX}{\beta} + \frac{m\,V\,dV}{\alpha\beta} + m\,dF = 0 \qquad (17)$$

This basic equation is now applied to the problem of gas-liquid flow in vertical pipes:

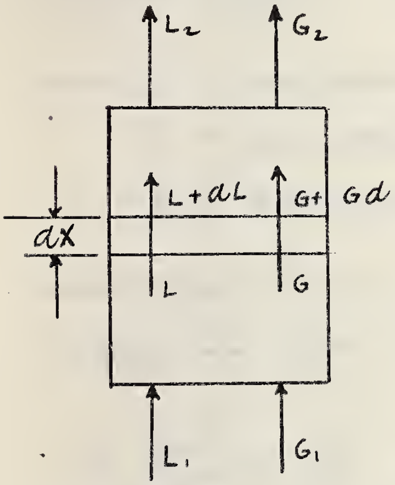

Let L = lbs/sec of liquid entering element dX

G = lbs/sec of gas entering element dX

$$L_1 + G_1 = L_2 + G_2 \qquad (18)$$

At the differential section dX for $d\theta\,G$ lbs. of gas

$$d\theta\left(G\,v_G\,dP + \frac{gGdX}{\beta} + \frac{GV_GdV_G}{\alpha_G\beta} + GdF_G\right) = 0 \qquad (19)$$

Similarly for $L\,d\theta$ lbs. of liquid

$$d\theta\left(L\,v_L\,dP + L\,\gamma_{L-G}\,d\sigma + \frac{gLdX}{\beta} + \frac{LV_LdV_L}{\alpha_L\beta} + L\,dF_L\right) = 0 \qquad (20)$$

combining equations (19) and (20) and dividing by L gives:

$$\left(\frac{G}{L}v_G + v_L\right)dP + \left(\frac{G}{L} + 1\right)dX\,\frac{g}{\beta} + \frac{1}{\beta}\left(\frac{GV_GdV_G}{L\alpha_G} + \frac{V_LdV_L}{\alpha_L}\right)$$

$$+ \gamma\,d\sigma + \frac{G}{L}\,dF_G + dF_L = 0 \qquad (21)$$

Assuming for a preliminary analysis that:

(a) the surface energy term $\gamma\,d\sigma$ is of negligible importance

(b) the kinetic energy term $\frac{1}{\beta}\left(\frac{G}{L}\;\frac{V_GdV_G}{\alpha_G} + \frac{V_LdV_L}{\alpha_L}\right)$

is of negligible importance

and calling $d\,F = \frac{G}{L}\,d\,F_G + d\,F_L$ (22)

then approximately,

$$\left(\frac{G}{L}\,v_G + v_L\right) d\,P + \frac{g}{\beta}\left(\frac{G}{L} + 1\right) d\,X + d\,F = 0 \qquad (23)$$

Now $v_G = \frac{Z\,R\,T}{P\,M}$ (24)

where Z = compressibility factor

R = gas constant

M = molecular wt.

Substituting (24) in (23) and integrating the expression and assuming $\frac{G}{L}$ inlet $\doteq$ $\frac{G}{L}$ discharge $\doteq$ $\frac{G}{L}$ average, gives

$$\left(\frac{G}{L}\,\frac{ZRT}{M}\right) \ln \frac{P_2}{P_1} + v_L\,(P_2 - P_1) + \frac{g}{\beta}\left[\left(\frac{G}{L}\right) + 1\right](X_2 - X_1) + \Delta F = 0 \qquad (24)$$

Now $P_{LM} = \frac{P_2 - P_1}{\ln \frac{P_2}{P_1}}$, so $\ln \frac{P_2}{P_1} = \frac{P_2 - P_1}{P_{LM}}$ (25)

where P_{LM} = log mean pressure

so equation (24) becomes

$$\left[\left(\frac{G}{L}\,\frac{ZRT}{M}\right)\frac{1}{P_{LM}} + v_L\right](P_2 - P_1) + \frac{g}{\beta}\left[\left(\frac{G}{L}\right)_{av.} + 1\right](X_2 - X_1) + \Delta F = 0 \qquad (26)$$

but $(v_G)_{LM} = \frac{ZRT}{M\,P_{LM}}$

where $(v_G)_{LM}$ = log mean specific volume of gas

assuming $(v_G)_{av.} \simeq (v_G)_{LM} \simeq \frac{ZRT}{M\,P_{LM}}$ equation (26)

becomes,

$$\left[(\frac{G}{L}\,v_G)_{av.} + v_L\right](P_2-P_1) + \frac{g}{\beta}\left[(\frac{G}{L})_{av.} + 1\right](X_2-X_1) + \Delta F$$

$$= 0 \qquad (27)$$

Dividing equation (27) by $\left[(\frac{G}{L}\,v_G)_{av.} + v_L\right](X_2-X_1)$ and transposing gives,

$$-\left(\frac{P_2-P_1}{X_2-X_1}\right) = \frac{g}{\beta}\,\frac{(\frac{G}{L})_{av.} + 1}{(\frac{G}{L}\,v_G)_{av.} + v_L} + \frac{\Delta F}{\Delta X\left[(\frac{G}{L}\,v_G)_{av.} + v_L\right]} \qquad (28)$$

This relation indicates that the pressure gradient, $-\frac{\Delta P}{\Delta X}$ may be considered to have two components. The first of these:

$$\frac{g}{\beta}\,\frac{(\frac{G}{L})_{av.} + 1}{(\frac{G}{L}\,v_G)_{av.} + v_L},$$ represents the hydrostatic

head per unit of height equivalent to the discharge mixture; while the second term,

$$\frac{\Delta F}{\Delta X\left[(\frac{G}{L}\,v_G)_{av.} + v_L\right]},$$ represents the irreversibility

effects per unit of height. The irreversibilities include wall friction effects, slippage between the air and water phases, the effects of holdup and flow pattern, energy required in forming gas bubbles and subdividing the liquid droplets, and other effects. This may be

written more simply as:

$$-\frac{\Delta P}{\Delta X} = \frac{\Delta P_H}{\Delta X} + \frac{\Delta P_F}{\Delta X} \qquad (29)$$

where, $-\frac{\Delta P}{\Delta X}$ = the actual pressure gradient

$\frac{\Delta P_H}{\Delta X}$ = the hydrostatic head component of the gradient

$\frac{\Delta P_F}{\Delta X}$ = irreversibility component of the gradient

III

EXPERIMENTAL EQUIPMENT

The experimental equipment designed for the vertical flow of air-water mixtures can be classified as follows:

1. Flow Circuit
2. Panel Board

1. Flow Circuit

The flow circuit, Figure 1, can be best discussed under the following headings:

a. Air supply
b. Water supply
c. Air control and measurement
d. Water control and measurement
e. Mixing section
f. Vertical flow sections
g. Back pressure control and discharge
h. Air purge

a. Air Supply--Air is supplied at 100 p.s.i. by an air compressor having a capacity of 120 c.f.m. A reducing valve inserted in the line gives a steady pressure of 60 p.s.i. All air piping fixtures between the air supply and mixing section are one inch unless noted otherwise.

b. Water Supply--Water is available at 23 p.s.i. from a constant level, overhead tank. If larger pressures are desired the water can be bipassed through a centrifugal pump having a capacity of 70 gallons per minute at 110 p.s.i. All water piping fixtures between the water supply and the mixing chamber are one inch unless noted otherwise.

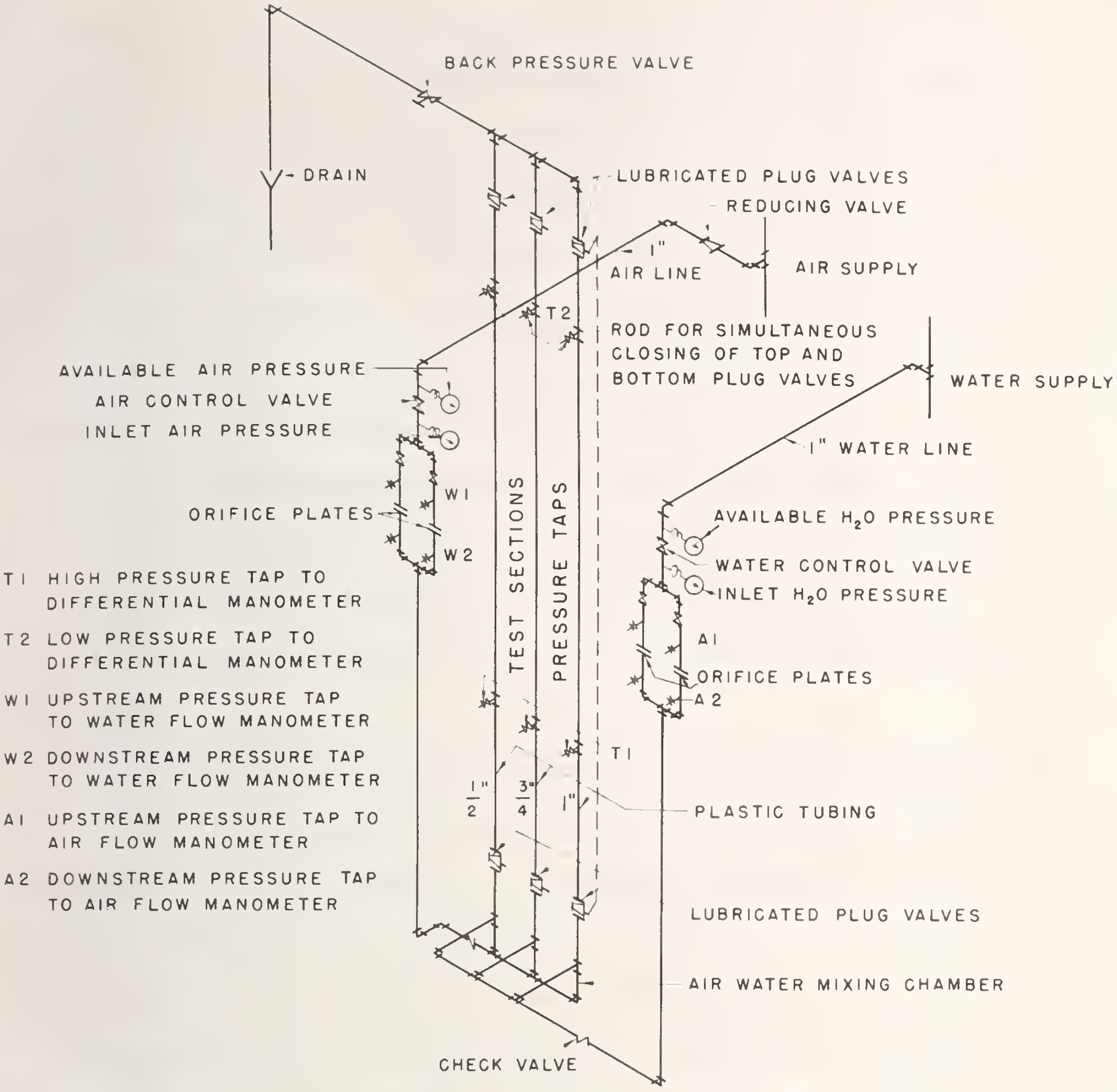

Figure 1

Flow Circuit

c. Air Control and Measurement--A one-inch, "plug disc", globe valve controls the volume of air. For finer control a 1/4" bipass line with a 1/4" needle valve is provided. Air flow is measured by an air flow manometer, (See Figure 2), connected to pressure taps located up and downstream of the orifice plate. In order to eliminate the necessity of frequently changing the orifice plates, two orifice unions are installed in parallel lines, (See Figure 3). The air flow manometer is connected to both sets of pressure taps.

d. Water Control and Measurement--The water control and measurement is identical to that discussed under the air control and measurement, that is, a one-inch "plug disc", globe control valve, and a water flow manometer connected to two sets of pressure taps on parallel orifice lines.

e. Mixing Section--The mixing sections are connected to the bottom of each vertical flow section. The air and water enter the mixing section from air and water headers. The mixing sections are merely vertically placed galvanized iron "T's", size 2" x 2" x 1". In each mixing section air enters the bottom two-inch branch, water the one-inch side branch, and the resulting air-water mixture flows through the top two-inch branch. The top of each of the mixing sections is connected by an appropriate reducer to a size of galvanized iron pipe corresponding to the plastic tubing above. (See Figure 4).

A two-inch reducer and two-inch union connect each mixing section with the one-inch air header. Ten two-inch diameter circular disks of 40-mesh screen are inserted in each union. These screens serve to disperse the air prior to mixing. Check valves are located upstream of both the air and water headers.

f. Vertical Flow Sections--There are three vertical flow sections (See Figures 1 and 5), sizes 1", 3/4" and 1/2", each extending vertically

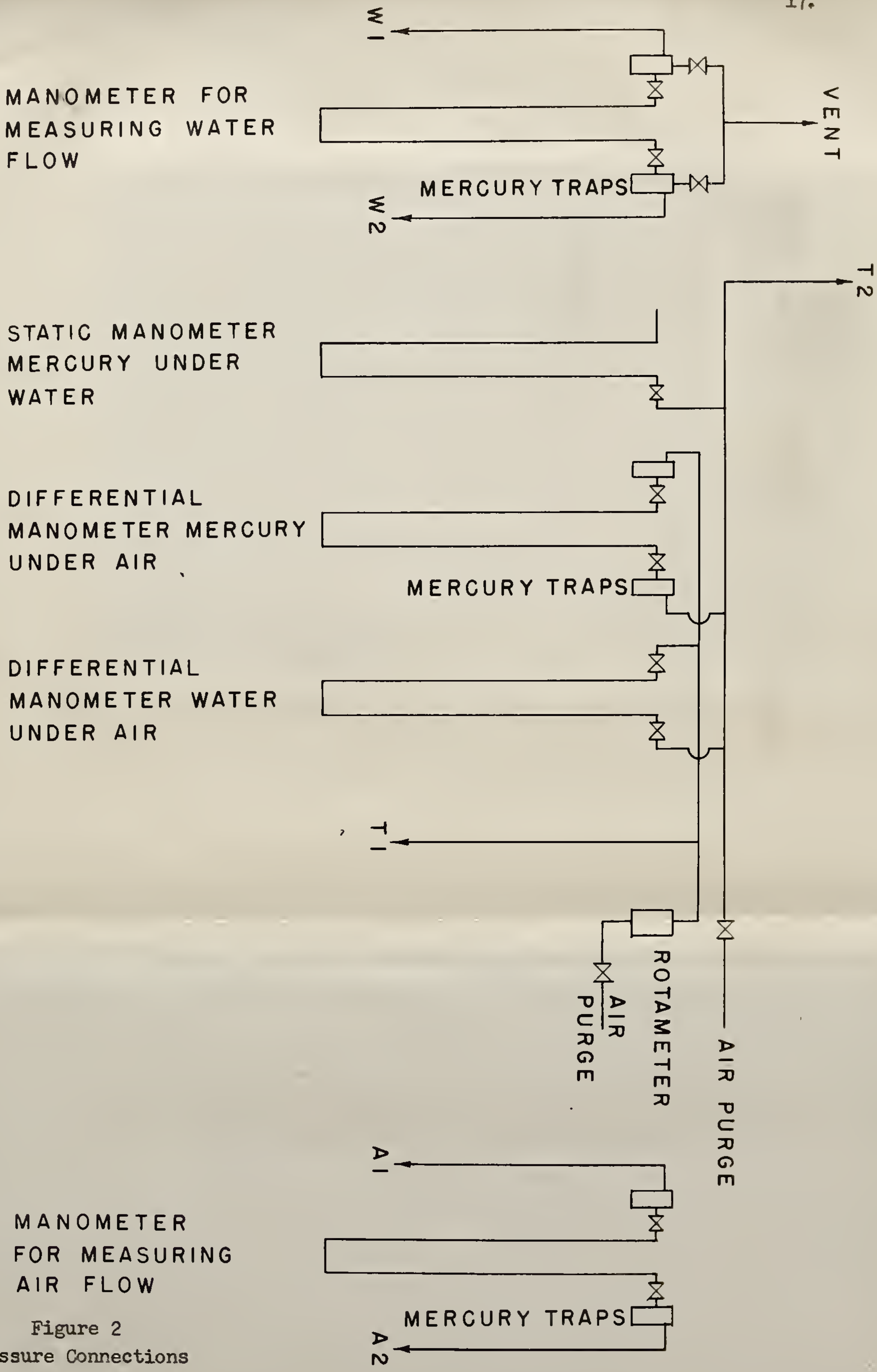
MANOMETER FOR MEASURING WATER FLOW
STATIC MANOMETER MERCURY UNDER WATER
DIFFERENTIAL MANOMETER MERCURY UNDER AIR
DIFFERENTIAL MANOMETER WATER UNDER AIR
MANOMETER FOR MEASURING AIR FLOW
W 1
W 2
VENT
MERCURY TRAPS
T 2
MERCURY TRAPS
T 1
ROTAMETER
AIR PURGE
AIR PURGE
A 1
A 2
MERCURY TRAPS

Figure 2
Pressure Connections

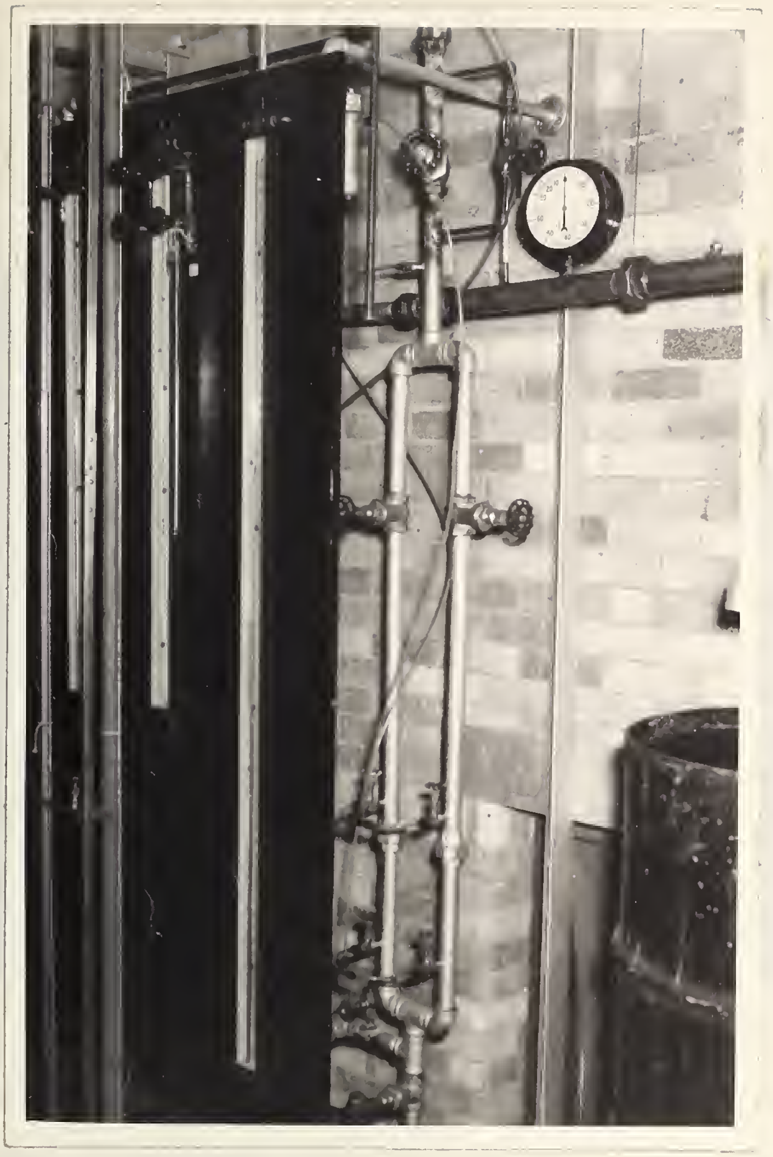

Figure 3

Panel Board and Air Measuring Section

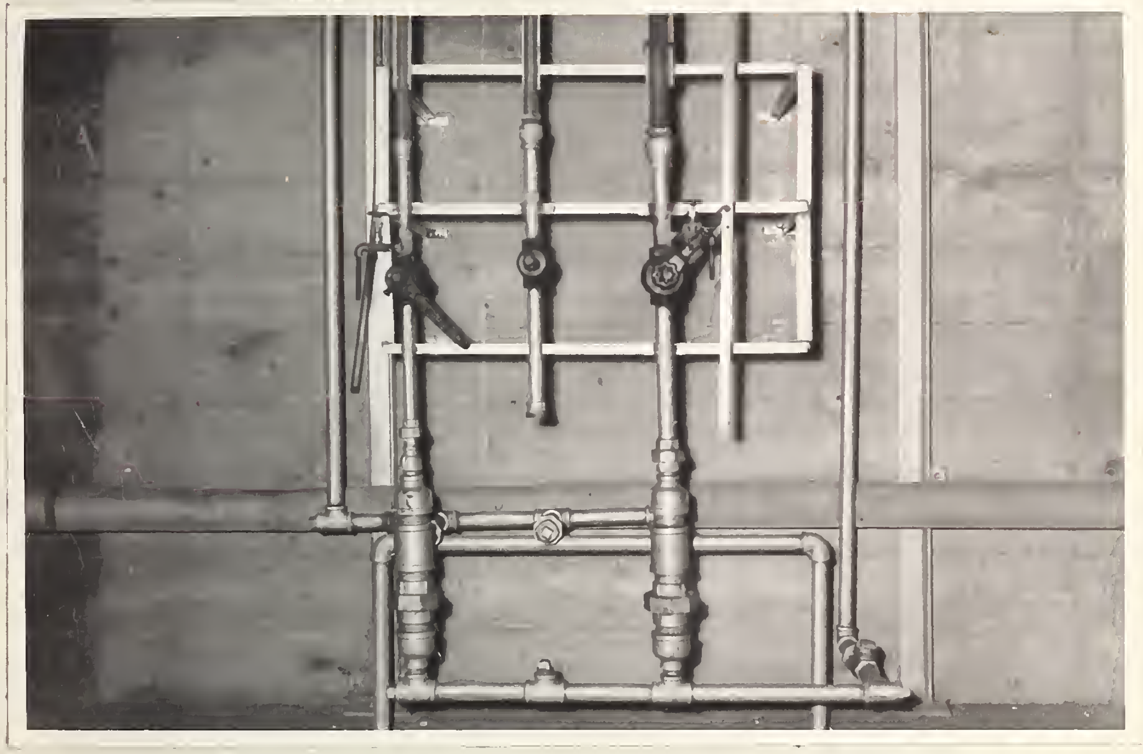

Figure 4

MIXING SECTIONS AND BOTTOM OF

VERTICAL FLOW SECTIONS

35 feet above the mixing section. The actual transparent plastic sections are each 30 feet long, and lie between 2½-foot sections of galvanized iron pipe. The size of these pipes corresponds to the size of the plastic tubing to which they are joined. Appropriately-sized lubricated plug valves are located in both the top and bottom sections of the galvanized pipe. The top and bottom plug valves of the flow section being used are interconnected by a 3/4-inch angle aluminum rod. By moving the rod up or down the top and bottom plug valves of the section being used can be opened or closed simultaneously. The actual inside diameters of the plastic in the three flow sections are 1.049", .824" and .640". Each plastic flow section contains two 15-foot lengths of clear butyrate tubing. In joining two sections of plastic tubing a close fitting plastic sleeve is slipped over the butted ends and then sealed to the tubes using chloroform.

In joining plastic tubing to a similar-sized section of galvanized iron pipe, a reducer is used. The small end of the reducer is screwed in the end of the galvanized pipe. (See Figure 6). The inside of the reducer is then machined so that the end of the plastic tube can be butted against the iron pipe inside the reducer. A split brass collar is fitted in a machined groove on the outer surface of the plastic tubing about ½" from the butted end. Above this is a snug-fitting bushing. Screwing the bushing in the reducer forces down on the collar thus insuring a snug fit between the butted ends of the plastic tubing and iron pipe.

The plastic flow sections are fitted flush in the "V's" of thirty-foot vertical sections of angle iron. Each angle iron section is spot welded to the grating of the floor levels and braced at the top and bottom to the wall.

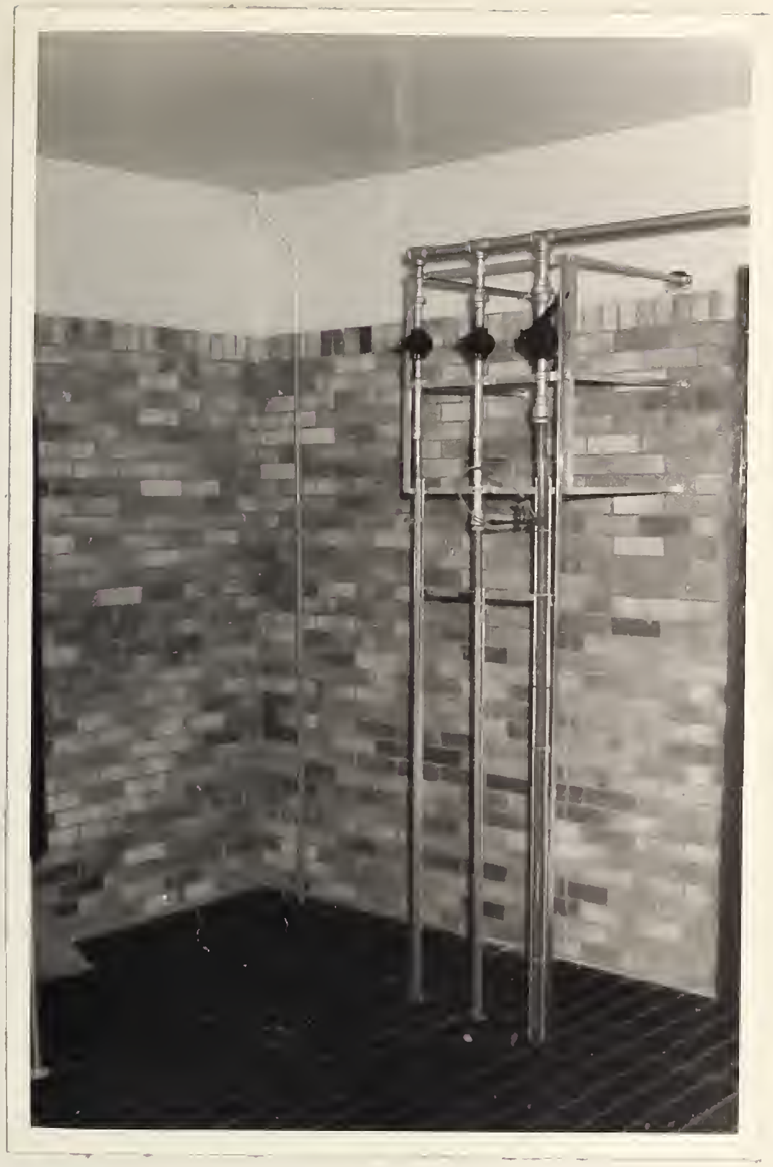

Figure 5

Upper Vertical Flow Section

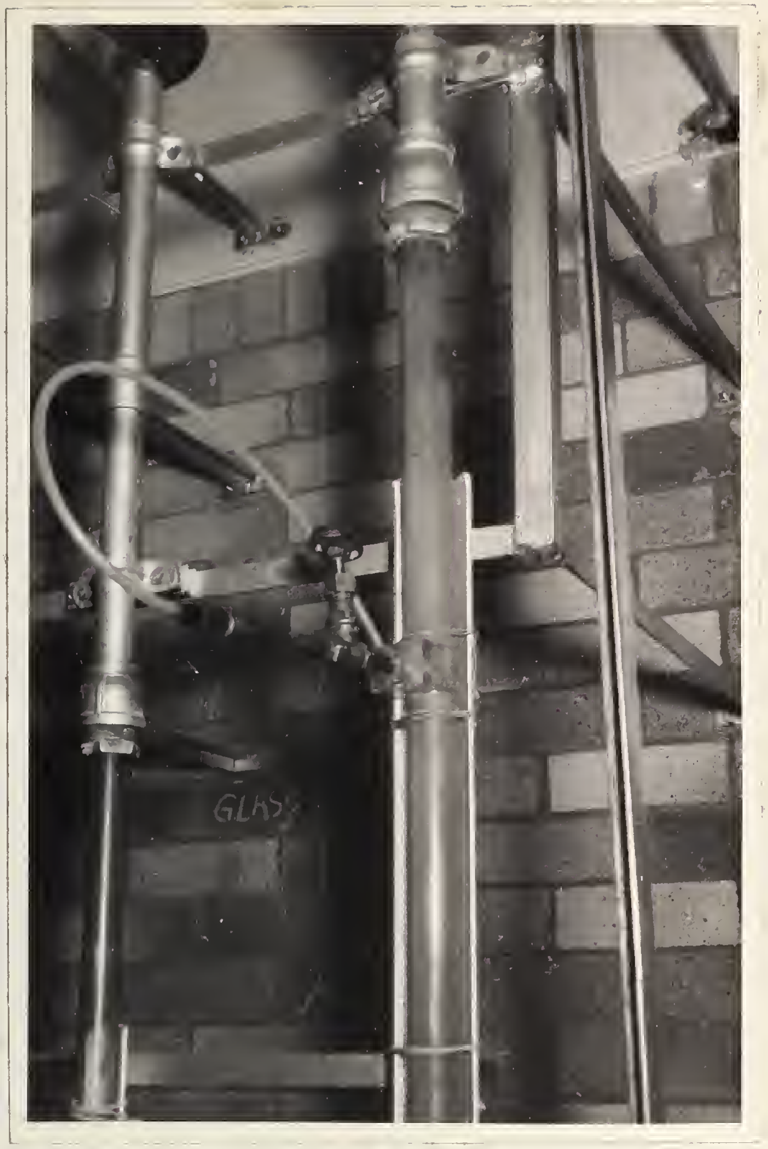

Figure 6

Plastic Pressure Tap and Connection

Between the Plastic Tubing and the Iron Pipe

The pressure drops are measured over a 22.88-foot section of plastic, the bottom pressure tap being eight feet above the mixing chamber. The pressure taps in the flow sections are blocks of lucite machined to fit the particular tube, see Figure 6. Each block has a hole bored and tapped for 1/8" fittings. A 3/16" hole is carefully drilled in the plastic tubing where the pressure station is desired. The plastic block is then placed on the tubing so that the 1/8" and 3/16" holes coincide. It is then sealed to the tube using chloroform.

g. Back Pressure Control and Discharge--The three vertical flow sections are connected at the top to a one-inch discharge header. Downstream of the discharge header a one-inch, "plug disc" globe valve permits the control of the pressure in the vertical flow sections.

The air-water mixture is discharged through a one-inch pipe passing two feet down into an open-ended vertical six-inch drain pipe. The air separates to the atmosphere and the water to the drain.

h. Air Purge--A continuous air purge through the differential pressure lines is necessary to keep the lines free of the air-liquid mixture passing through the test section. The air purge flowing through the bottom pressure tap is metered by the use of a rotameter because it increases the amount of air flowing through the test section.

2. Panel Board

The panel board, Figure 7, is situated on the same level as the control valves. The three vertical flow sections pass flush in front of the panel board. Five manometers, Figure 2, and five pressure gauges are also located on the panel board.

The air and the water rates are measured by two five-foot Meriam manometers containing mercury under air and mercury under water,

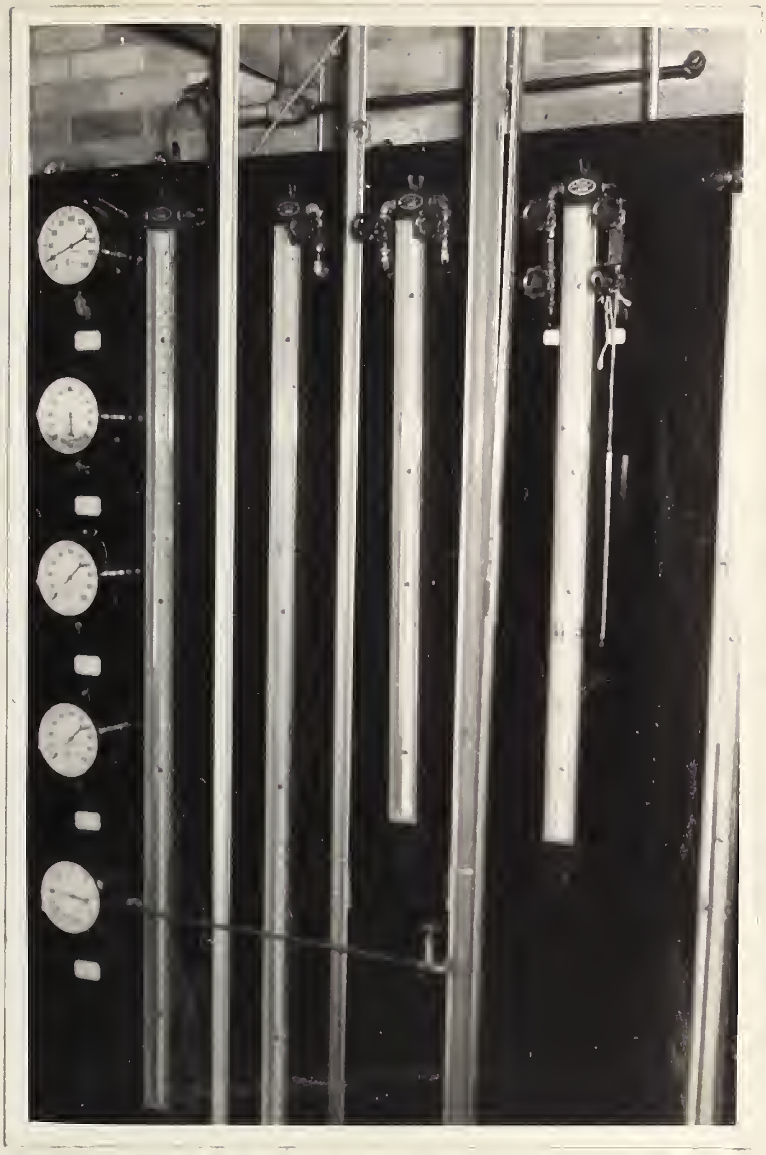

Figure 7

Panel Board

respectively. These are connected to pressure taps located up and downstream of the air and water orifice plates. The differential pressure drops are measured by two 76 cm. Meriam manometers, one containing mercury under air and the other water under air. These are both connected to the top and bottom pressure taps of the test section being measured. (See Figures 1 and 2). The static pressure is measured by a five-foot Meriam manometer containing mercury under air and connected to the top pressure drop tap.

All manometers containing mercury have mercury traps, Figure 8, inserted in the pressure leads just before they connect to the manometers. These traps prevent the mercury being blown from the manometer into the system. The mercury traps for the water flow manometer have vents at the top of each trap to permit "de-airing".

The available and inlet air pressures are measured by two pressure gauges connected above and below the air control valve. The water pressures are measured by two similarly-connected pressure gauges. The fifth pressure gauge is connected horizontally to a pressure tap at the mid point of the test section being used. This gauge gives a direct reading of the average pressure in the line.

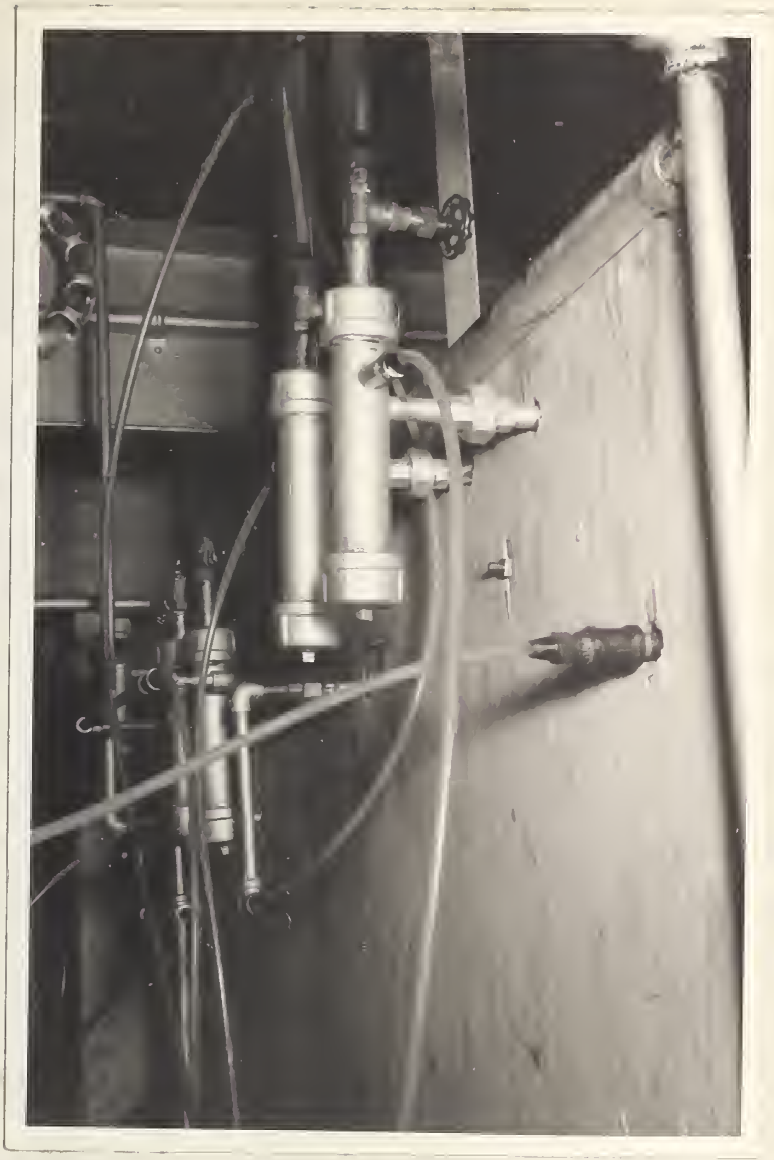

Figure 8

Mercury Traps (Rear of Panel Board)

IV

EXPERIMENTAL PROCEDURES

Several series of constant water rate tests were made, and for each series the air rate was varied from zero to a maximum. The same experimental technique was followed for each test.

With both plug valves open the water present was drained from the vertical flow section using the 1/8" 'needle' globe valve 1/2" above the lower plug valve. When the test section was free of water, the 1/8" 'needle' valve was closed and the air purge through the bottom pressure tap was set at an adequate rate. The 1/4" 'needle' valve controlling the upper air purge was then opened until the manometers measuring the pressure drop registered zero differential.

When the air purge was correctly adjusted the two valves above the water orifice plates were opened. Then the water control valve was opened to permit "de-airing" of the water line. The valves above the mercury traps of the water flow manometer were opened to permit "de-airing" of the pressure leads. When "de-airing" was complete the valve above the orifice not being used was closed along with the pressure taps in the same line. A water rate slightly higher than desired was then set. With the water and air purges flowing through the system, the air control valve was carefully opened until the desired air rate was attained. The water rate was then reduced to the desired rate and, if necessary, a final adjustment on the air rate was made.

If a certain pressure in the flow section was desired, the back-pressure valve was adjusted. A rod connected to the valve handle permitted pressure control from the panel board level.

Conditions were kept constant for five minutes before the readings were taken. Then the readings of the water flow manometer,

the air flow manometer, the pressure drop manometer and static manometer were all recorded. Similarly, the inlet air pressure, the average pressure of the system, the barometer reading, the air temperature and the air-water mixture temperature were all noted.

Having made the necessary readings the rod connecting the top and bottom plug valves was briskly pulled down. After allowing the water five minutes to settle, the level of the water in the tube was recorded. The exact volume between the plug valves was previously determined and marks corresponding to 100 c.c. intervals were etched in the plastic tube. The last 200 c.c.'s of volume were in the galvanized iron pipe section separating the plastic tube from the plug valve. When the volume of the water was less than 200 c.c.'s it was drained and measured.

With the completion of the test the rod connecting the top and bottom plug valves was raised and a new test was carried out in a similar manner.

V

EXPERIMENTAL DATA

The experimental data are presented in Tables I - IV of Appendix A and in Tables V - XV of Appendix B. The data in Appendix A deal with calibrations, and those in Appendix B with the actual experimental tests.

(1) Appendix A

Table I contains data for the calibration of the water orifice plates. The run number is listed in Column 1. Column 2 records the amount of water discharged, (ft.^{3}), during the time interval listed in Column 3 as minutes and seconds. The water discharged was measured using a Pittsburgh water meter. The differential across the water flow manometer is reported in Column 4 as inches of mercury under water. Column 5 contains the calculated water rate, ft^3/sec. A plot of the water rate versus the manometer differential for each orifice plate is presented in Figure 10.

Table II presents data for the calibration of the air orifice plate constants using a critical flow prover. The number of the air orifice plate being calibrated is listed in Column 1. The upstream air orifice pressure p.s.i.,ga. and the differential across the air flow manometer inches of mercury under air, are reported in Columns 2 and 3 respectively. The temperatures, degrees absolute, and pressures, p.s.i.,ga. upstream of the critical flow prover are listed in Columns 4 and 5. Column 6 contains the size of the critical flow prover and Column 7 the critical flow coefficient of the prover.

The results calculated from the data in Table II are listed in Table III. The air orifice plate number is reported in Column 1. The actual flow rates, 1000 ft^3/day, are presented in Column 2. These

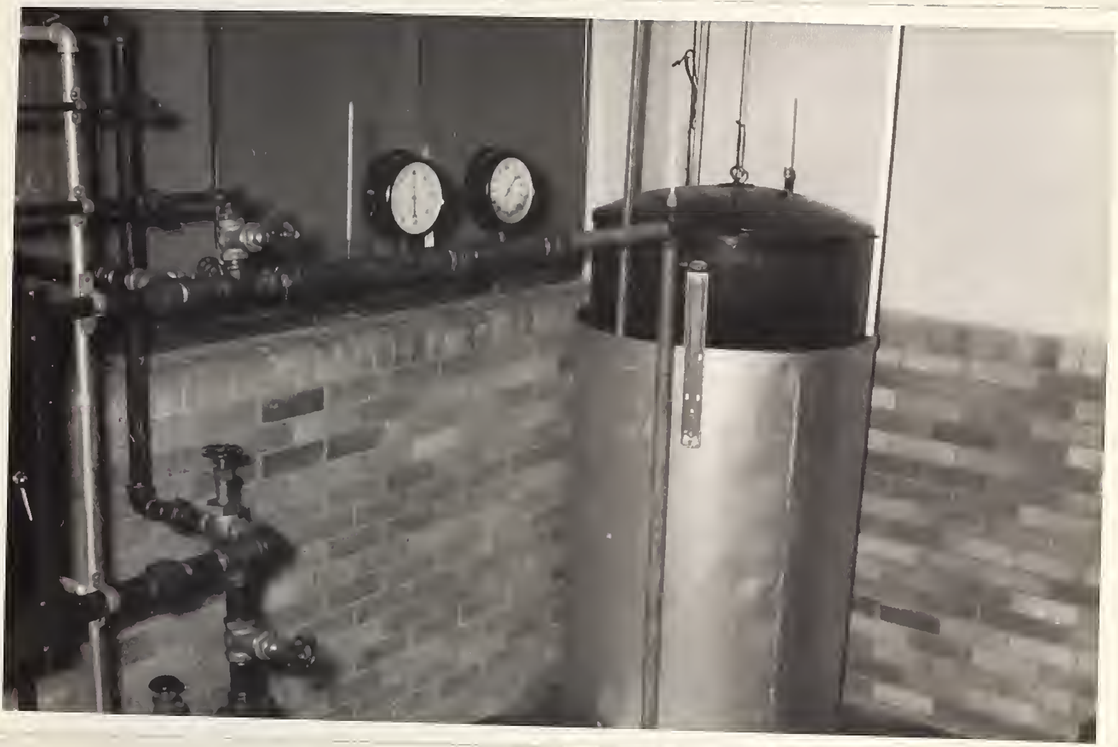

Figure 9

Critical Flow Prover

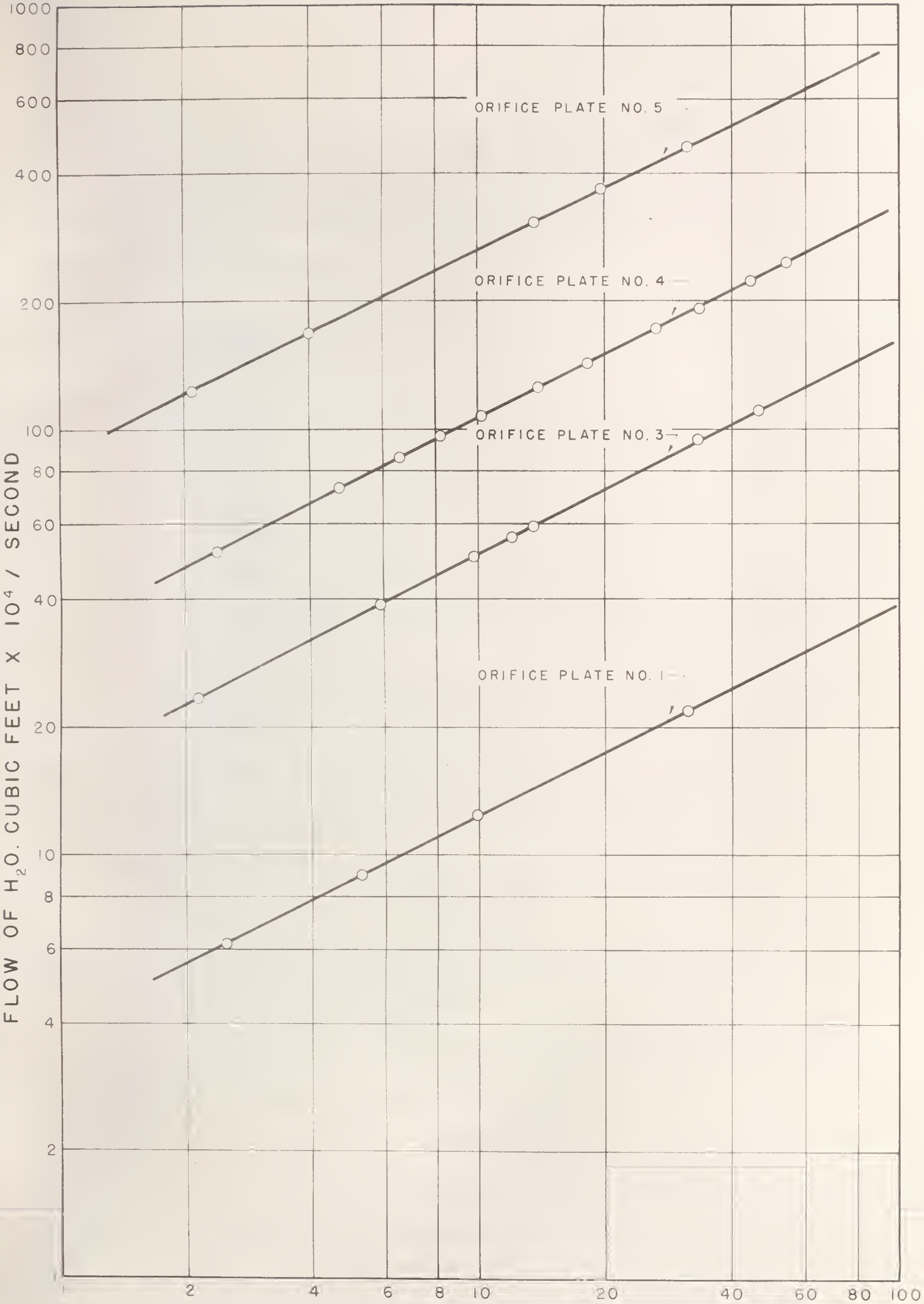

Figure 10

Water Orifice Plate Calibration Data

were calculated using the equation from the U.S. Department of the Interior, Bureau of Mines booklet entitled, "Back Pressure Data on Natural Gas Wells and their Application to Production Practices". The gas rate is defined as:

$$Q_c = \frac{C\,P}{\sqrt{G'\,T}} \qquad (30)$$

where, Q_c = rate of flow 1000ft^3/24 hrs. at 14.4 p.s.i.a. and 60°F.

C = critical flow coefficient

P = upstream pressure p.s.i.a.

G' = specific gravity of the gas

T = the upstream temperature of the flowing gas (degrees Rankine)

The air rates converted to ft^3/sec are reported in Column 3 and the air orifice plate constants, "K", are listed in Column 4. These constants were calculated from the equation in the booklet, "Orifice Meter", Pittsburgh Meter Company, where for the discharge of gas through an orifice,

$$Q_o = K\sqrt{\frac{h_m P_f}{T_f}} \qquad (31)$$

where Q_o = air rate ft^3/sec, at 14.4 p.s.i. abs. and 16° F.

K = air orifice constant

h_m = differential manometer reading, inches of mercury under air

P_f = upstream air pressure p.s.i.a.

T_f = air temperature degrees Rankine.

Table IV lists the experimental data and calculated results for the calibration of the rotameter used in measuring the air purge through the bottom pressure tap of the test section. Columns 1,2, and 3, respectively, contain the test numbers, the rotameter readings and the air temperatures, °F. Column 4 records the amount of air discharged

ft^3 during the time interval listed in Column 5 as seconds. The air discharged was measured with a wet test meter. The calculated air rates, ft^3/sec, are contained in Column 6 and these rates, converted to ft^3/sec at 14.4 p.s.i.a. and 60°F, are reported in Column 7. The calibration of the rotameter is only valid for 14.4 p.s.i.a. and 60°F. All readings made at other pressures or temperatures must be multiplied by

$$\sqrt{\frac{P_r\,520}{14.4\,T_r}}$$

(This correction is listed in a Schutte and Koerting pamphlet for the University of Alberta) (32)

where, P_r = pressure of the air passing through the rotameter, p.s.i.a.

T_r = temperature of the air passing through the rotameter, °A.

(2) Appendix B

Table V contains supplementary data giving the length of the test section, the type of tube and its inside diameter.

Tables VI-VIII contain experimental water flow data. The test number is indicated in Column 1 and the water temperature °F. in Column 2. Column 3 shows the water rate which was measured using a water flow manometer connected to pressure taps up and downstream of a calibrated orifice plate. Pressure drop data are presented in Column 4 which shows the manometer differential in cms. of the manometer fluid indicated. The temperature of the air surrounding the air manometer is reported in Column 5.

Experimental data for the air-water tests are presented in Tables IX - XV. Each table represents a series of tests made at a different constant water rate. Column 1 lists the test number and Column 2 the air temperature °F. The total air rate, ft^3/sec, is recorded in Column 3. This total includes the air entering the mixing

section, and the air purge entering the bottom pressure tap of the test section. The main air rate is measured using an air flow manometer and the purge rate by use of a rotameter. The water rate shown in Column 4 is measured by a water flow manometer. Column 5 lists the average pressure drop in the line P.S.I.A. The measured pressure drop cm. of mercury under air, is recorded in Column 6. The volume of air in the flow section for each run is listed in Column 7 and the volume of water is contained in Column 8.

VI

CALCULATED RESULTS

The important results calculated from the original data are presented in Tables XVI - XXVII of Appendix C.

Tables XVI - XVIII list the results of the series of water runs made to check the measuring technique and smoothness of the test section. Column 1 contains the test number. The measured pressure drops converted from cm. of manometer fluid to feet of water are listed in Column 2. Column 3 records the velocity of the water for each test. The calculated Reynolds number, $\frac{DVe}{\mu}$, is shown in Column 4. The friction factors, "f", are defined by equation (14) as $f = \frac{F \rho D}{2V^2 N_e}$, are listed in Column 5. A plot of the friction factor versus the Reynolds number is shown in Figure 11. The Kármán-Prandtl resistance equation for turbulent flow in smooth pipes was used for comparison. The curve was calculated using the equation defined in (5) by,

$$\frac{1}{\sqrt{f}} = 2 \log_{10} \text{Re.} \sqrt{f} - .8 \qquad (33)$$

where Re. = Reynolds number = $\frac{DVe}{\mu}$

Tables XIX - XXV contain the important results calculated from data for the series of air-water tests made. The test numbers are found in Column 1. Column 2 lists the air-water discharge ratio ft^3 at standard conditions per ft^3. The ratios in Column 2 were calculated by dividing the total measured air rate by the measured water rate on the assumption that the air-water ratio entering and leaving the test section was the same. Column 3 contains the air-water ratio in the test section ft^3/ft^3. These values were calculated by dividing the volume of air by the volume of water between the top and bottom plug valves.

Column 4 contains the total air rate, "G", converted to lbs/sec. and Column 5 the water rate, "L", converted to lbs/sec. The average specific volume, "v_G", of the air in the test section is listed in Column 6. Column 7 reports the "discharge" hydrostatic head defined by equation (28) as:

$$\frac{\left(\frac{G}{L}\right)_{av.} + 1}{\left(\frac{G}{L} v_G\right)_{av.} + v_L}, \text{ converted to p.s.i./100ft.}$$

The measured pressure drop converted to p.s.i./100ft. is listed in Column 8. Plots showing the measured pressure drop versus the air-water discharge ratio are presented in Figures 15 - 21.

Using equation (3) defined by $-\Delta P_{LH} = y \rho_L H$, the hydrostatic head for each test in Series A was calculated and converted to p.s.i./100 ft. The measured pressure drop p.s.i./100 ft. minus the converted hydrostatic head is reported in Column 9, Table XIX. A plot of the values of Column 9 versus the air-water discharge ratio is shown in Figure 12.

Table XXVI contains data from Figure 13 showing the variations of "holdup" with air-water discharge ratios. A plot of these values is presented in Figure 14.

The values of the pressure drops and air-water discharge ratios corresponding to each maximum and minimum point in Figures 15 - 21 are shown in Table XXVII. The constant water rates are listed in Column 1. Columns 2 - 4 list the pressure drops and air-water discharge ratios for each maximum and minimum point as follows:

Column 2 - the minimum points corresponding to "slugging" flow.

Column 3 - the maximum points corresponding to "froth" flow.

Column 4 - minimum points corresponding to "film" flow.

A plot of the values in Table XXVII is presented in Figures 21 and 22.

VII

INTERPRETATION AND CORRELATION OF RESULTS

The plot, Figure 11, of the friction factor versus the Reynolds number for pure water shows the calculated values closely follow the Kármán-Prandtl resistance equation for turbulent flow in smooth pipes. This indicates the test section can be considered smooth and the measuring technique is satisfactory.

In Figures 12 and 15-21 the measured pressure drops are plotted versus the air-water discharge ratios. These plots for the seven constant water rates show the same general trend over the range studied. The measured pressure drop curve in Figure 12 is useful in discussing the trends of the curves in detail.

At zero air rate the measured pressure drop is the hydrostatic head of water plus the frictional effects of the flowing water, i.e., a total of 43.5 p.s.i./100 ft. Introducing air to the flowing water results in a rapid decrease in pressure to a minimum pressure drop of 5.2 p.s.i./100 ft. occurring at an air-water discharge ratio of 95. The pattern of flow in the portion of this region observed is characterized by a series of alternate bullet-shaped air slugs, separated by "pistons" of water. Around each air slug an annular ring of water flows downwards. Therefore as the air slugs rise they progressively merge into larger ones. The size of the air slugs at any one section becomes larger with increasing air rates, reaching a maximum at an air-water discharge ratio corresponding to the first minimum.

Above an air-water discharge ratio of 95 the measured pressure drop increases to the first maximum of 7.2 p.s.i./100 ft. at an air-water discharge ratio of 210. During this increase the water "pistons"

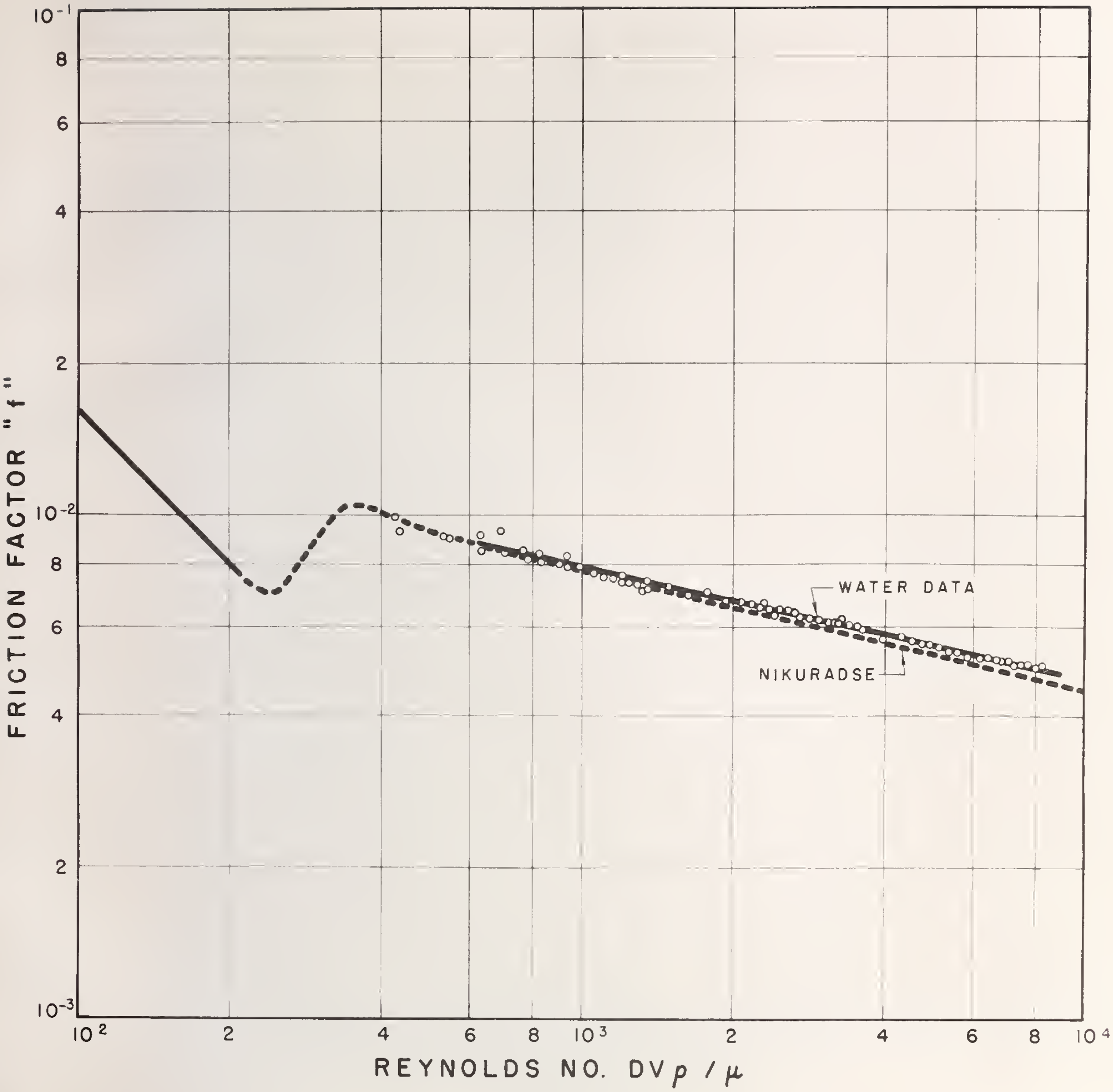

Figure 11

Water Test Data

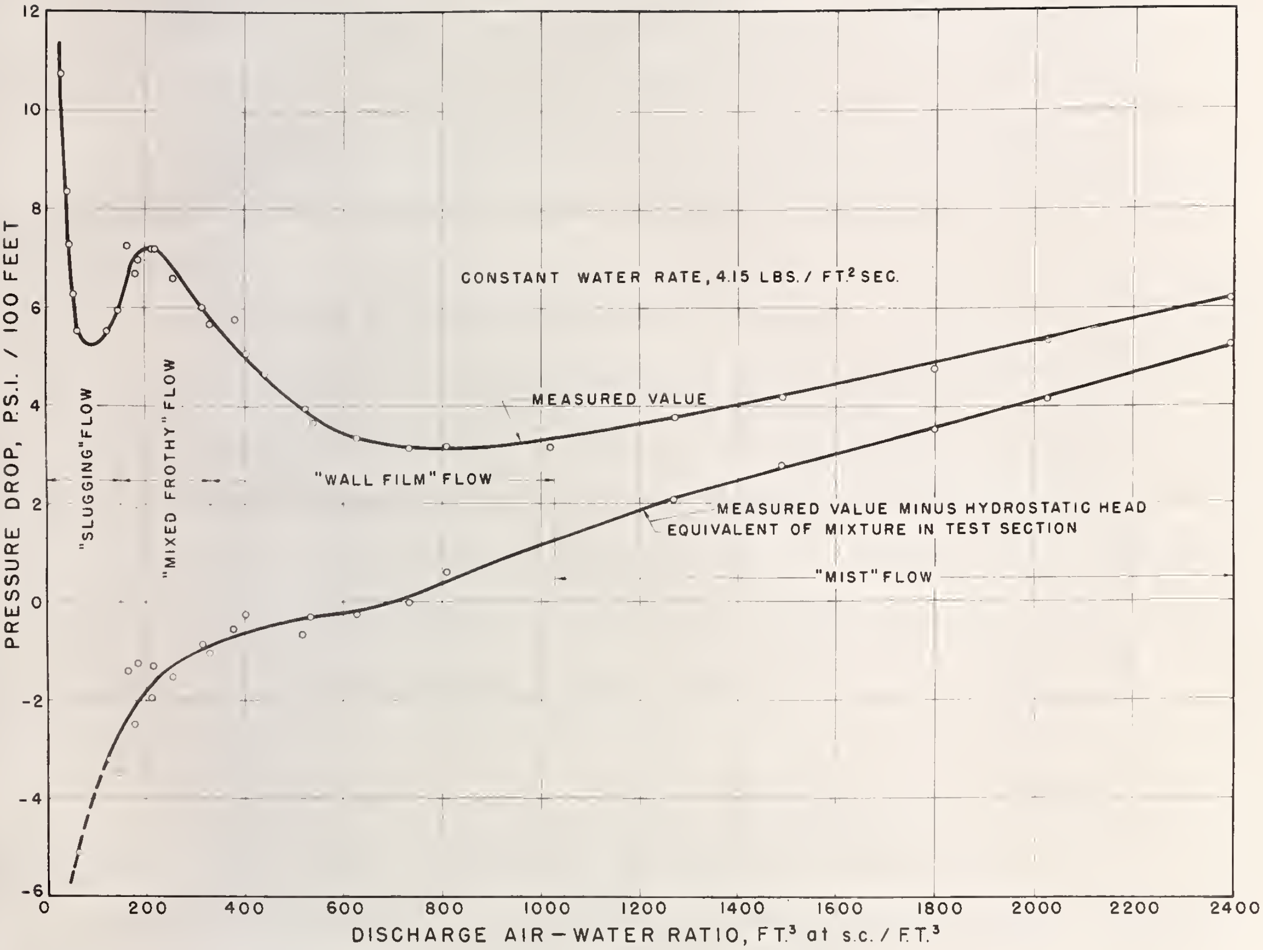

Figure 12

Effect of the Discharge Air-Water Ratio on the Pressure Drop
Showing the Hydrostatic Head Equivalent of the Mixture
in the Test Section

become dispersed with small air bubbles and the bullet-shaped air slugs become less distinct. At an air-water discharge ratio corresponding to that of this maximum the flow is pulsating and "frothy" in appearance. There are rapidly flowing alternate pistons of "froth" separated by air slugs. Around each air slug a frothy annular ring flows downwards. In the seven constant water rate series conducted the most violent pulsations appeared to occur at a discharge air-water ratio corresponding to the maximum point on the measured pressure drop curve.

As the air rate is further increased, the measured pressure drop decreases to a second minimum of 3.05 p.s.i./100 ft. at an air water discharge ratio of 825. This pressure decrease is accompanied by a gradual transition in the flow pattern—from "frothy" flow to "film" flow. "Film" flow is characterized by a core of mist flowing through an annular film of water moving upwards at a slower rate. The second minimum measured pressure drop occurs in the region of "film" flow.

At ratios in excess of 825, on increasing the air rate, the water film gradually disappears and the tube becomes filled with rapidly flowing mist. In the region of mist flow the measured pressure drop increases smoothly with increased air rate.

Not only were the general shapes of the other six measured pressure drop curves the same, but the flow patterns corresponding with the same portions of the curve were similar.

In the literature review it was stated that it appears doubtful if the equation (3), $-\Delta P_{LH} = y \rho_L H$, is valid in the calculation of the hydrostatic head effect. However, as a check, values for this equation from tests in series 1 were converted to p.s.i./100 ft. and subtracted from the measured pressure drop p.s.i./100 ft.

These values, Column 9, Table XIX, are plotted versus the air-water discharge ratio in Figure 12. The hydrostatic head using equation (3) is greater than the measured pressure drop up to air-water discharge ratios of 700. For flowing mixtures the measured pressure drop includes hydrostatic head effect plus frictional effects. Therefore the measured pressure drop for flowing mixtures must exceed the hydrostatic head. It may therefore be seen that the relationship proposed by Moore and Wilde (4) is not valid in the low gas-liquid discharge ratio range.

The general thermodynamic approach indicates that the pressure gradient may be considered as the sum of two components. These are the hydrostatic head equivalent of the discharge mixture and the irreversibilities related to the mechanism of flow. Using equation (28) the discharge hydrostatic heads, Column 7, Tables XIX - XXV, were calculated for each series on the basis of p.s.i./100 ft. These hydrostatic head equivalents of the discharge mixture were plotted versus the air-water discharge ratios along with the measured pressure drops in Figures 15-21. These curves may be better discussed after a consideration of the "holdup" relationships.

The air water ratios in the test section for the series of air-water runs were plotted versus the air-water discharge ratios. A typical plot is presented in Figure 13.

In the discussion of theory it was shown that the test-section air-water ratio was dependent on the discharge air-water ratio and on the relative velocity of the air to water. Calling the air-water discharge ratio "D", and the test section air-water ratio "T", the theoretical considerations indicate the following.

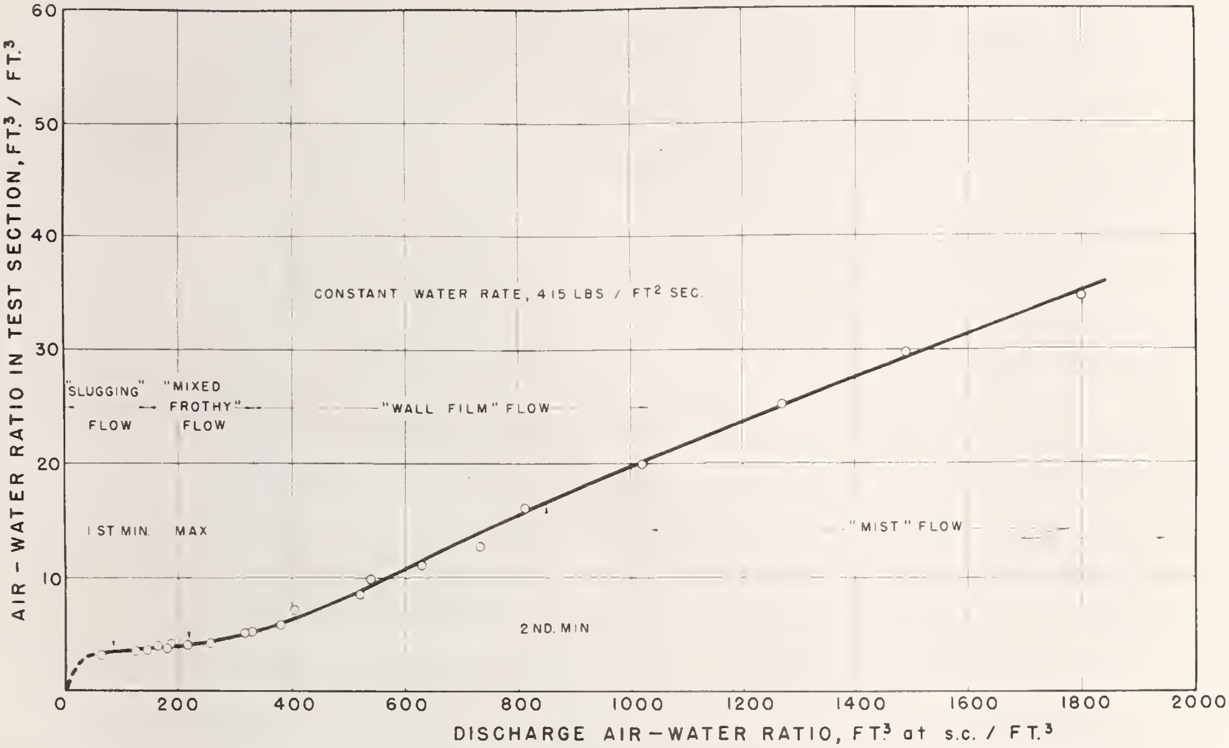

Figure 13

Effect of the Discharge Air-Water Ratio on the Air-Water Ratio in the Test Section

An increase in D at a constant relative velocity between the air and water has no effect on the ratio, $\frac{D}{T}$; whereas an increase in the relative velocity of air to water at constant D increases the ratio $\frac{D}{T}$. Therefore, a variation of the ratio $\frac{D}{T}$ with D indicates a change in the relative velocity of the air to water.

Using the values from Figure 13, shown in Table XXVI, a plot, Figure 14, was made of the ratio $\frac{D}{T}$ versus D, the air-water discharge ratio. Figure 14 indicates that $\frac{D}{T}$ increases between ratios of 50 and 350. Therefore between these ratios the relative velocity of the air to water is increasing. This region corresponds to the "froth" flow pattern. In the region of "film" flow, corresponding to discharge ratios 350 to 1000, $\frac{D}{T}$ decreases indicating a decrease in the relative velocity of the air to the water. This is the first region where all the water flows upward; that is, there is no downward flow.

In ratios in excess of about 1000, $\frac{D}{T}$ is observed to be nearly independent of the discharge ratio. This may be taken as evidence that the relative velocity of the air to water is nearly constant.

Knowing where and in which direction the relative velocity changes it is possible to discuss Figures 15-21 with a clearer understanding. The measured pressure gradient has been shown to be equivalent to a hydrostatic head effect and to a "friction" or irreversibility effect related to the flow mechanism. These irreversibilities include friction between the mixture and the wall, "slippage" between the air and water phases moving at different velocities, energy required in forming gas bubbles and subdividing the liquid droplets, changes in

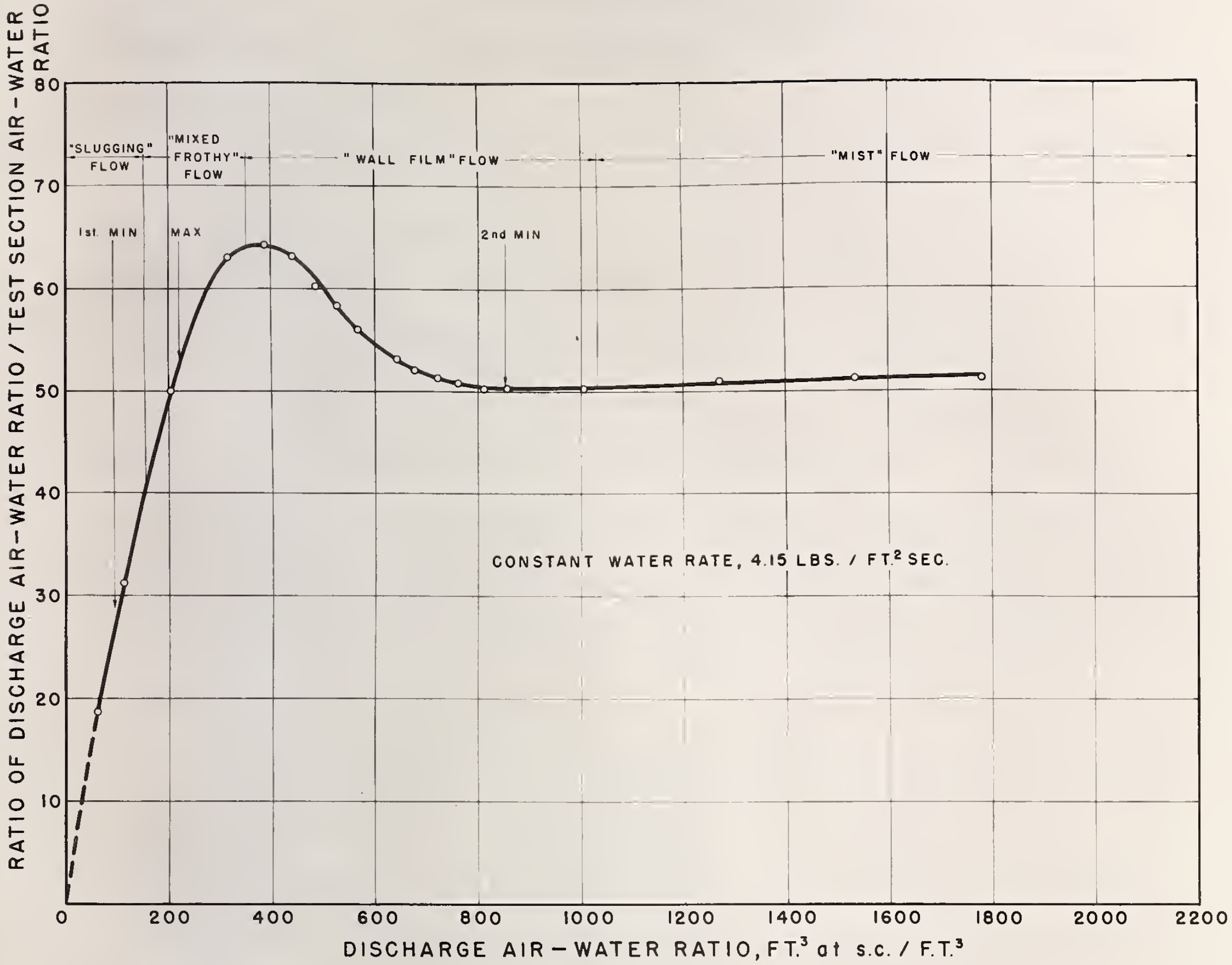

Figure 14

Effect of the Discharge Air-Water Ratio on the

Ratio of the Discharge to the Test Section Air-Water Ratio

velocity head and others. The viscosity and interfacial area vary for different gas-liquid ratios and flow patterns but the importance of these effects is not known. Figure 15 is useful in interpreting the significance of the shape of the curves and especially the maximum and minimum points.

The initial decrease in the measured pressure drop is due largely to the rapid decrease in the "discharge" hydrostatic head. The rate of decrease of the hydrostatic head, however, falls off sharply as the first minimum is approached. At the same time the relative velocity of the air to water is rapidly increasing and it appears valid to assume that the "slippage" portion of the friction is increasing at a corresponding rate. Where the rate of increase of "slippage friction" exceeds the rate of decrease of hydrostatic head, the measured pressure drop starts to increase, that is, the first minimum occurs.

At air-water discharge ratios beyond the first minimum, the discharge hydrostatic head effect is small. The increase of the measured pressure drop to the maximum point is largely due to the rapid increase in slippage between the air and water and to the development of other irreversibilities due to the change in flow pattern. In the maximum region the flow is extremely pulsating and frothy in appearance.

The transition to "film" flow is accompanied by a decrease in pressure to the second minimum and a decrease in the relative velocity of the air to water. During the change in flow pattern from "frothy" to "film" flow there is a gradual transition from pulsating to comparatively smooth flow. The discharge hydrostatic head and the wall friction of the slowly moving annular ring are both negligible effects. Therefore the decrease in pressure drop appears due to the decrease

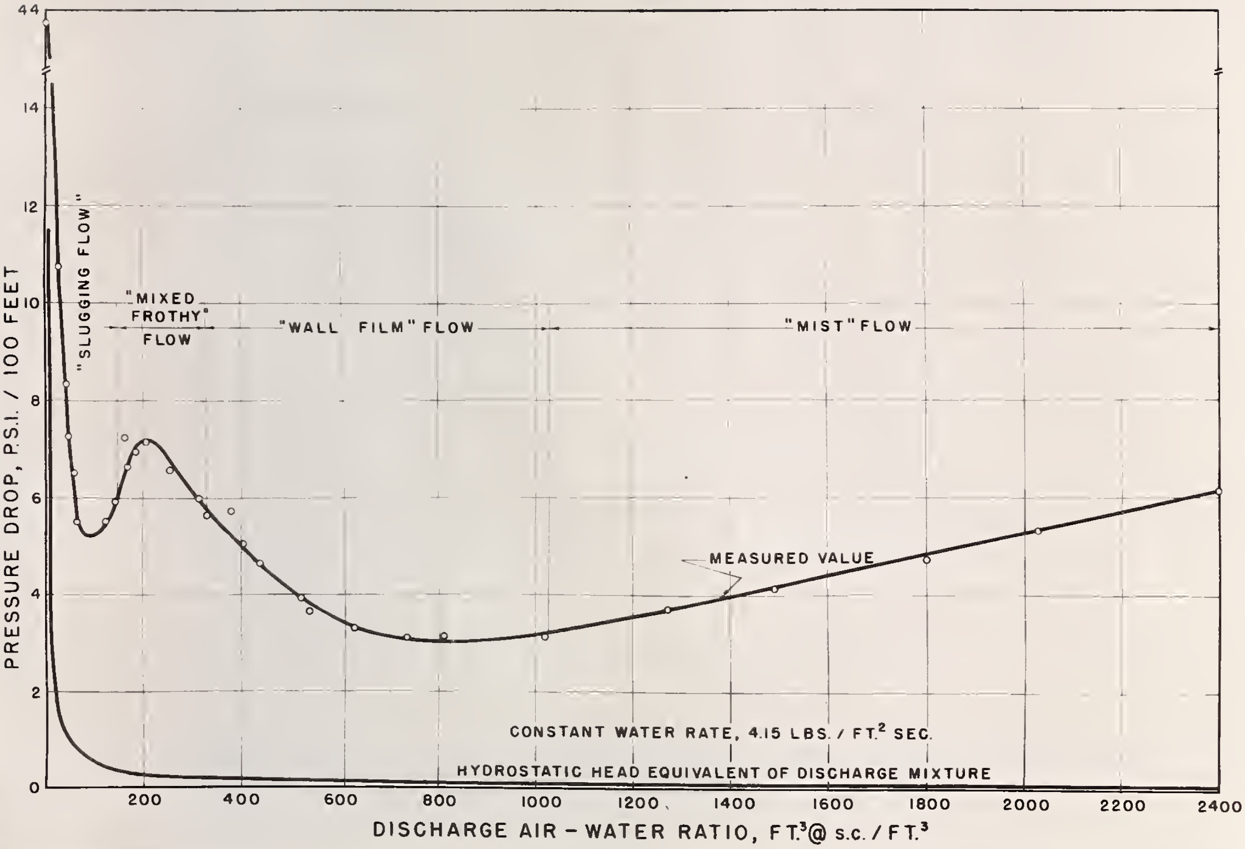

Figure 15

Effect of the Discharge Air-Water Ratio on the Pressure Drop Showing the Hydrostatic Head Equivalent of the Discharge Mixture

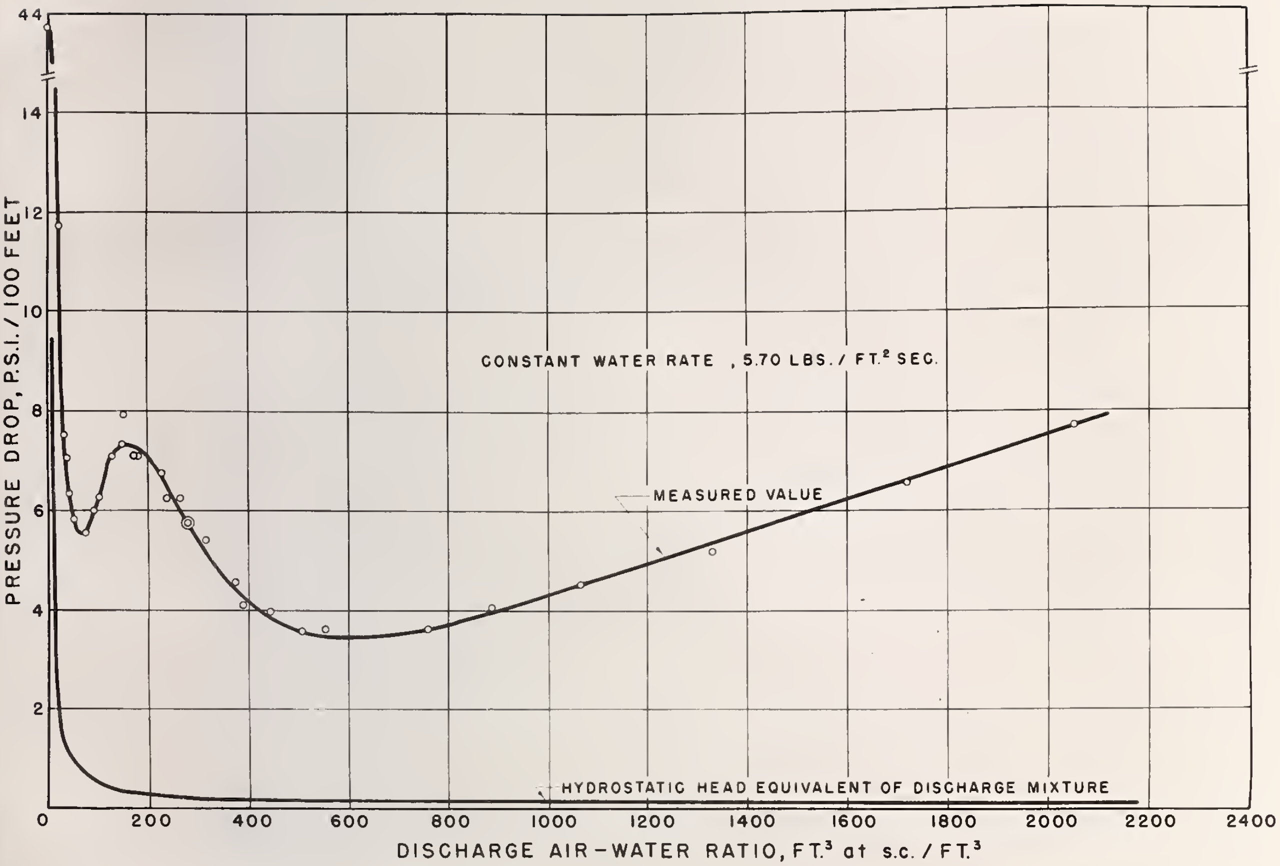

Figure 16

Effect of the Discharge Air-Water Ratio on the Pressure Drop Showing the Hydrostatic Head Equivalent of the Discharge Mixture

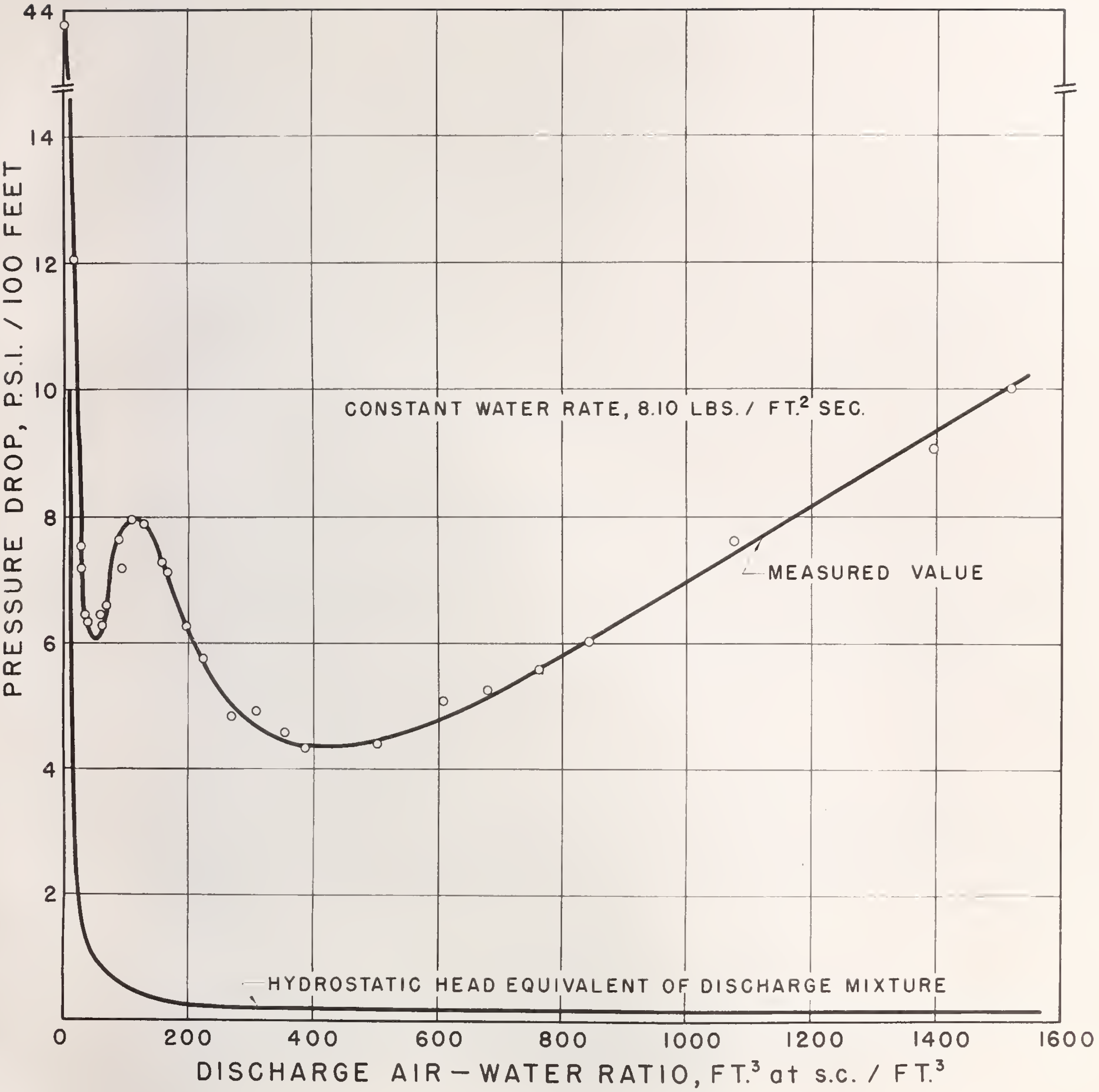

Figure 17

Effect of the Discharge Air-Water Ratio on the
Pressure Drop Showing the Hydrostatic Head Equivalent
of the Discharge Mixture

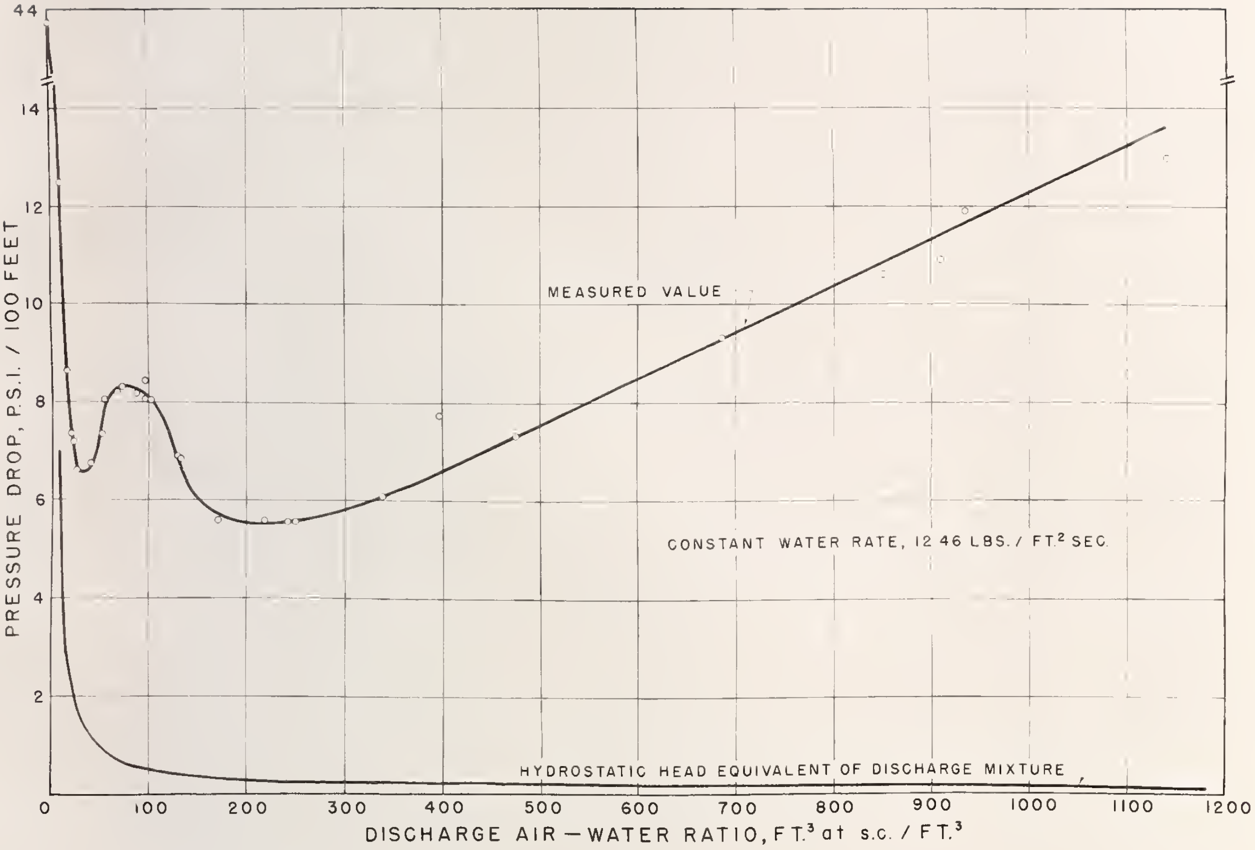

Figure 18

Effect of the Discharge Air-Water Ratio on the Pressure Drop Showing the Hydrostatic Head Equivalent of the Discharge Mixture

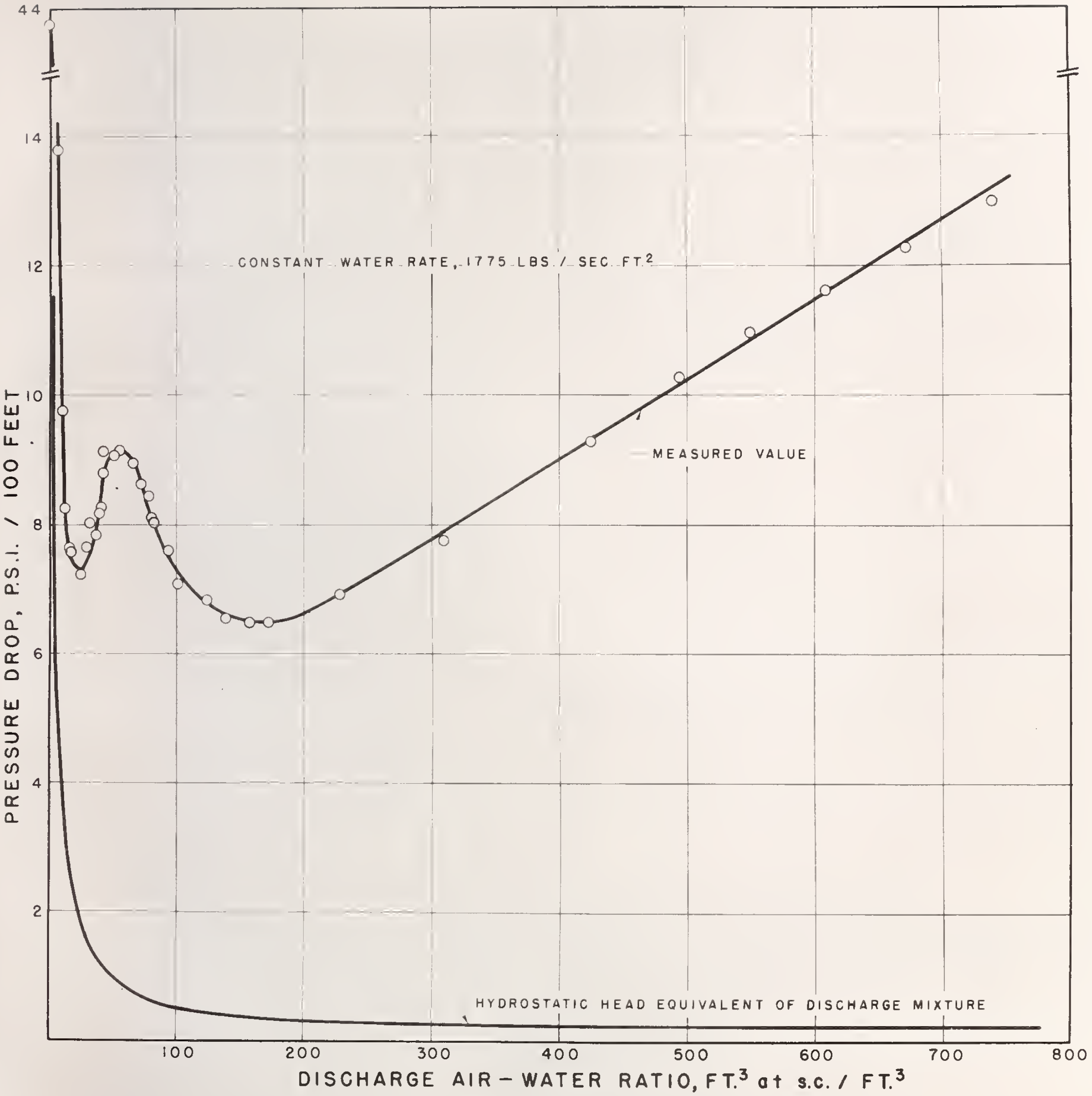

Figure 19

Effect of the Discharge Air-Water Ratio on the Pressure Drop Showing the Hydrostatic Head Equivalent of the Discharge Mixture

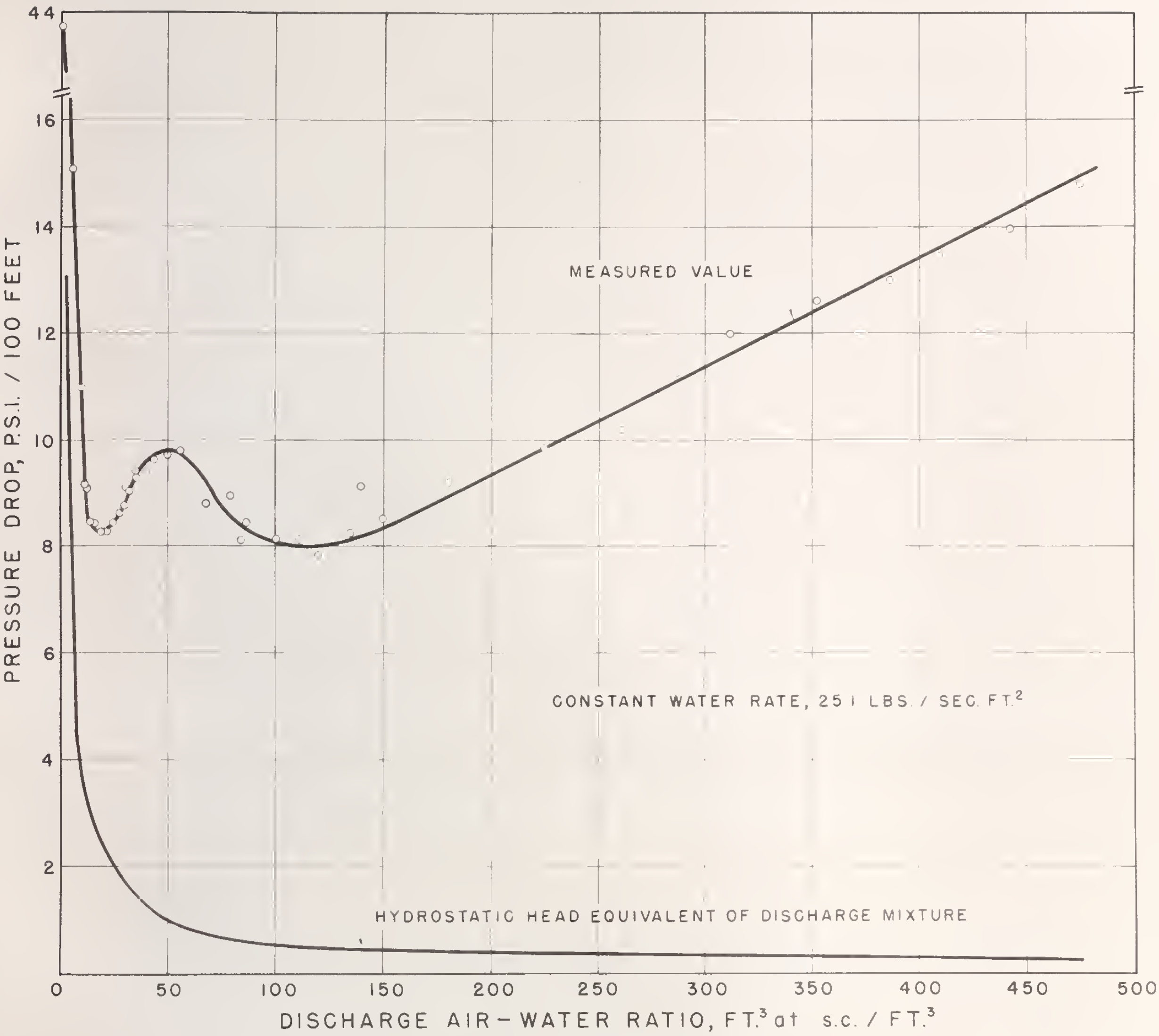

Figure 20

Effect of the Discharge Air-Water Ratio on the Pressure Drop Showing the Hydrostatic Head Equivalent of the Discharge Mixture

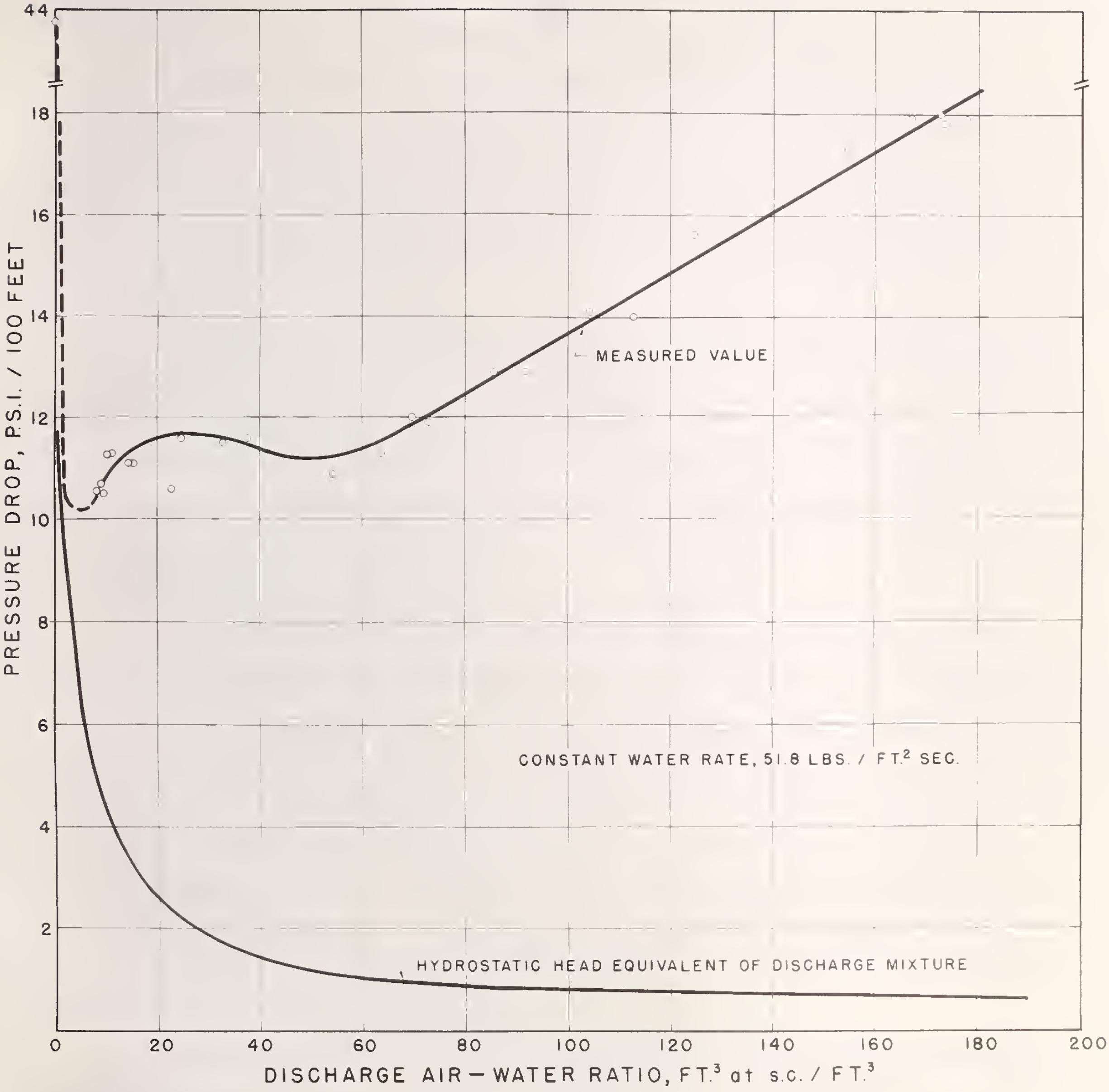

Figure 21

Effect of the Discharge Air-Water Ratio on the Pressure Drop Showing the Hydrostatic Head Equivalent of the Discharge Mixture

in slippage between the two phases and to other irreversibilities relative to the new mechanism of flow.

In the region of "mist" flow the pressure drop increases smoothly with increasing air rate. Since the relative velocity of the air to water is fairly constant and the discharge hydrostatic head effect negligible, it appears likely that the predominating factor is wall friction.

Pressure drops and air-water discharge ratios corresponding to each of the maximum and minimum points of Figures 15-21, are presented in Table XXVII. The results are shown graphically in Figures 22 and 23, and illustrate the changes of the measured pressure drops and the air-water discharge ratios with water rate.

Figure 22 indicates that the maximum and minimum pressure drops increase with increased water rates. At higher water rates this trend is less pronounced. The "froth" maximum and the "film" minimum curves approach each other as the water rate is increased. Therefore it seems reasonable to assume that at some higher water rate the "froth" maximum and the "film" minimum may disappear leaving only the one minimum point--that is, the "slug" minimum. The confirmation of this is given by the actual data.

At water rates below 36 lbs/ft^{2}sec the pressure drop corresponding with the "slug" minimum is higher than that for the "film" minimum. At water rates greater than 35 lbs/ft^{2}sec the "slug" minimum pressure drop is lower than that for the "film" minimum. This indicates that at higher rates, where the "froth" maximum and "film" minimum may disappear, the only minimum point will occur in the "slug" flow region.

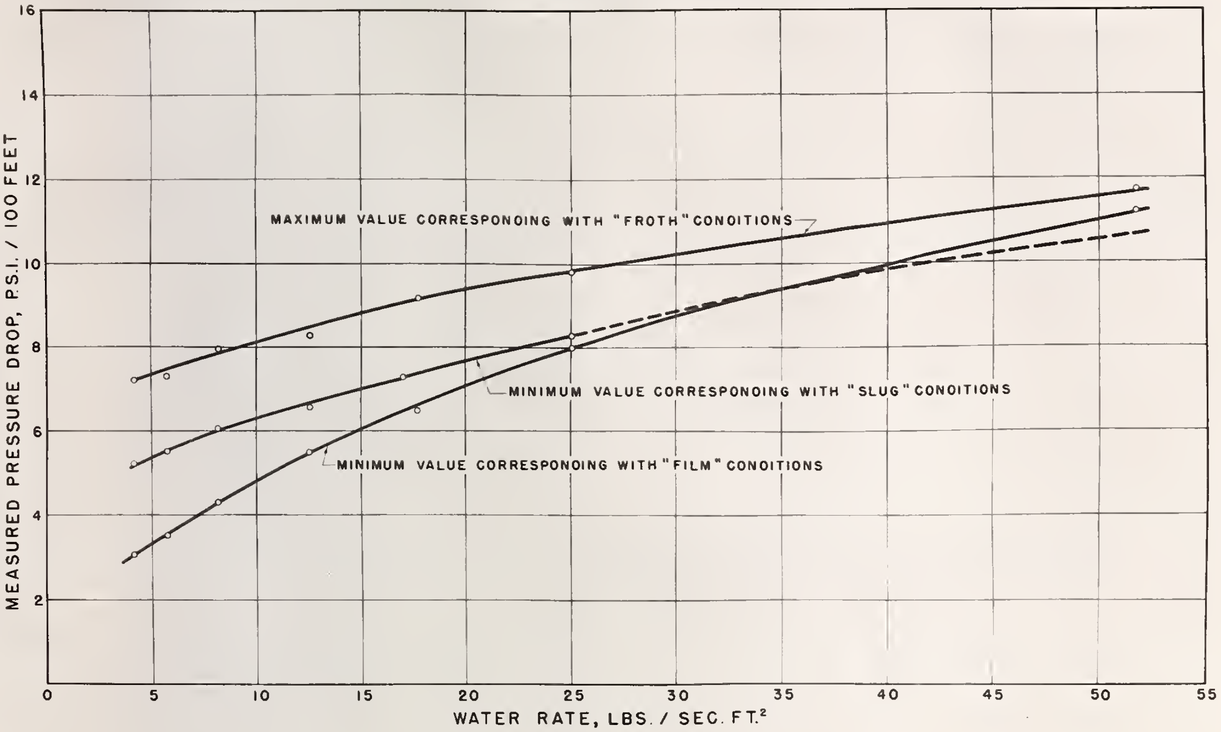

Figure 22

Effect of the Water Rate on the
Maximum and Minimum Pressure Drops

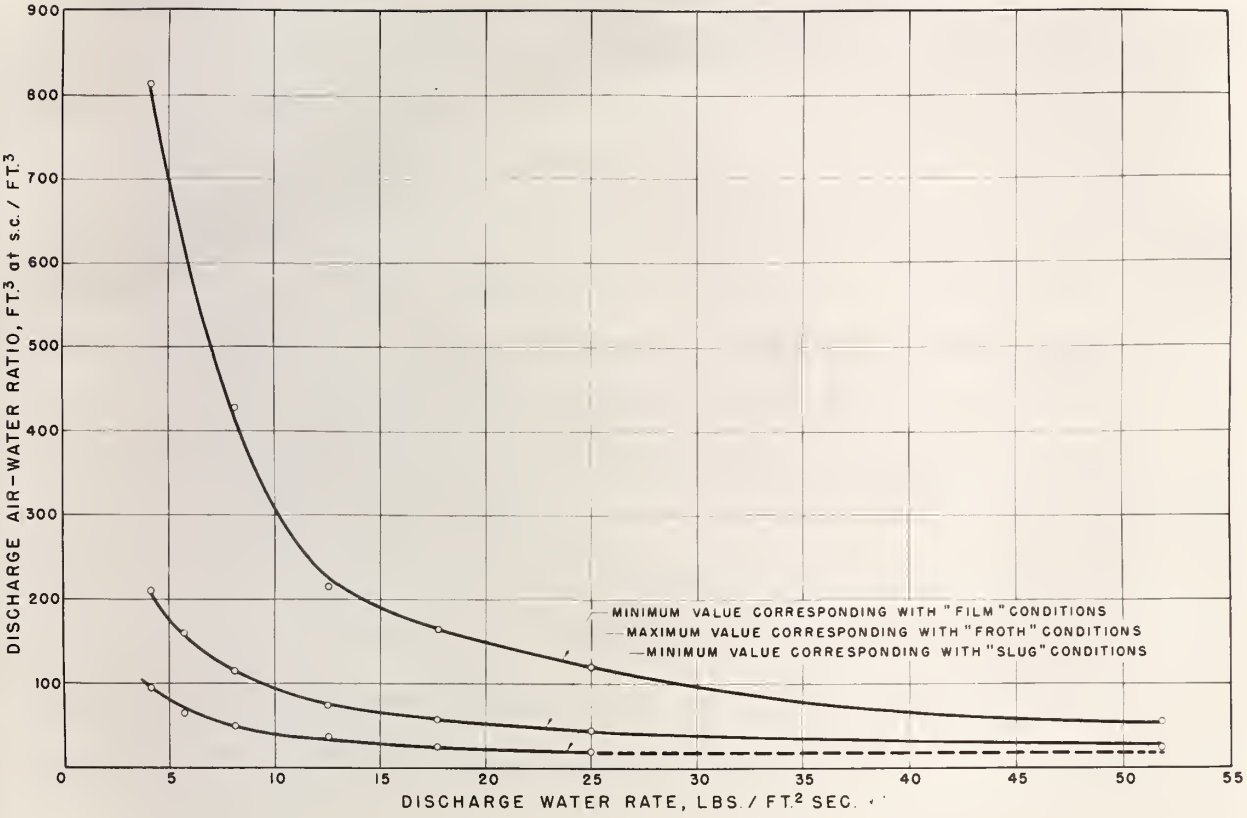

Figure 23

Effect of the Water Rate on the Air-Water Ratios Corresponding with the Maximum and Minimum Pressure Drops

Figure 23 indicates that the air-water discharge ratio at which the minimum and maximum points occur, decreases when the water rate is increased. This phenomenon, however, is much more pronounced at lower water rates.

While the evidence is not conclusive, it appears that the air rates at which the maximum and minimum points occur are independent of the water rate. (See Table XXVIII). Likewise, for the "slug" minimum and the "froth" maximum, the holdup in the tube as indicated by the air-water ratio in test sectin was approximately the same for the different water rates investigated. However, for the "film" minimum, the holdup in the tube increased at higher water rates. Since the pressure drops for the "slug" minimum and "froth" maximum are greater at higher water rates but the air-water ratio in the tube is constant, the difference in pressure must be attributed to the difference in the discharge hydrostatic heads and the irreversibilities of flow. This offers some justification to the procedure of considering the pressure gradient in terms of the two components--hydrostatic discharge and irreversibilities.

VIII

CONCLUSIONS

1. A versatile experimental unit for the study of pressure drops for the flow of gas-liquid mixtures through vertical pipes has been designed, constructed and successfully operated.

2. For the seven constant water rates studied, as the air rate is increased, the measured pressure drop passes through a first minimum point, a maximum point, a second minimum and then increases at a smooth rate.

3. The flow pattern changes with increased air rates from "slug" flow, to "froth" flow, to "film" flow, to "mist" flow. This transition is closely related to the changes in the measured pressure drop curve.

4. The region of the first minimum is found to be characterized by "slug" flow--bullet shaped air slugs separated by pistons of water. The first minimum is the result of a rapid decrease in the hydrostatic head effect.

5. The maximum region is characterized by frothy, pulsating flow. The relative velocity of the air to water increases rapidly in the transition from the minimum to the maximum pressure point. This indicates that slippage between the air and the water phases is the predominant frictional effect.

6. "Film" flow occurs in the region of the second minimum pressure drop. It is characterized by a core of mist flowing through an annular film of slower moving water. The relative velocity of the

air to the water decreases during the change from the maximum to the minimum pressure point.

7. At higher air rates the liquid film disappears, that is, the tube is filled with rapidly flowing mist. In the region of "mist" flow the pressure drop increases smoothly with increased air rates. The relative velocity of the air to the water is fairly constant, and it appears that wall friction is the predominant factor in the pressure gradient.

8. The equation $-\Delta P_{LH} = y \rho_L H$ is found invalid at low air-water discharge ratios.

9. The experimental data indicate that at higher water rates the "froth" maximum and the "film" minimum disappear leaving only a "slug" minimum.

10. The investigation indicates the need for a detailed study of the irreversibilities and their relation to the flow pattern, the system geometry, the fluid properties, etc. It is possible that the irreversibilities may be treated by the use of a modified "friction factor" and Fanning-type equation. Since the flow pattern appears dependent mainly on the air rate this suggests that a modified Reynolds number based on the air rate might be used.

APPENDIX A

CALIBRATIONS

TABLE I

EXPERIMENTAL DATA

CALIBRATION OF WATER ORIFICE PLATES

Orifice Plate No. 1

1	2	3			4	5
Run No.	Discharge	Time			Manometer Difference	Rate
	Ft^3	Min.		Sec.	Inches Hg. under H_2O	Ft^3/Sec
1	.50	15	-	05	2.20	.000553
2	.25	6	-	50	2.50	.000610
3	1.00	18	-	31	5.25	.000900
4	.60	8	-	01	9.95	.00125
5	1.00	7	-	52	29.70	.00209
6	.50	3	-	48	31.50	.00219

Orifice Plate No. 3

1	2	3			4	5
Run No.	Discharge	Time			Manometer Difference	Rate
	Ft^3	Min.		Sec.	Inches Hg. under H_2O	Ft^3/Sec
1	1.00	4	-	17	5.90	.00389
2	1.00	3	-	19	9.80	.00503
3	1.00	3	-	00	12.10	.00560
4	2.00	5	-	37	13.65	.00593
5	1.00	1	-	46	33.25	.00943
6	1.00	1	-	30	46.20	.0111

TABLE I (CONT.)

EXPERIMENTAL DATA

CALIBRATION OF WATER ORIFICE PLATES

Orifice Plate No. 4

1	2	3		4	5
Run No.	Discharge	Time		Manometer Difference	Rate
	Ft.^{3}	Min.	Sec.	Inches Hg. under H_2O	Ft^3/Sec
1	1.00	3 -	13	2.40	.00518
2	1.00	2 -	17	4.70	.00730
3	1.00	1 -	56	6.55	.00863
4	2.00	3 -	28	8.20	.00967
5	2.00	3 -	06	10.25	.01075
6	2.00	2 -	38	14.00	.0126
7	2.00	2 -	19	18.25	.0144
8	3.00	2 -	53	26.55	.0173
9	3.00	2 -	35	33.65	.0194
10	3.00	2 -	15	44.40	.0224
11	3.00	2 -	02	54.20	.0246

Orifice Plate No. 5

1	2	3		4	5
Run No.	Discharge	Time		Manometer Difference	Rate
	Ft.^{3}	Min.	Sec.	Inches Hg. under H_2O	Ft^3/Sec
1	3.00	4 -	03	2.10	.0124
2	3.00	2 -	58	4.00	.0169
3	4.00	2 -	10	13.65	.0308
4	4.00	1 -	49	19.60	.0369
5	5.00	1 -	48	31.15	.0461

TABLE II

EXPERIMENTAL DATA

AIR ORIFICE CALIBRATION USING CRITICAL FLOW PROVER

Barometer Rdg. 27.60" Hg.

1 Air Orifice No.	2 Pressure Upstream of Air Orifice p.s.i.ga	3 Manometer Difference ins-Hg. under air	4 Temp. Upstream Critical Orifice ° Abs.	5 Pressure Upstream Critical Flow Orifice p.s.i.ga.	6 Size of Orifice Prover ins.	7 Critical Flow Coefficient
1	27.5	13.45	535.0	21.10	3/32	3.59
1	37.5	16.45	535.0	28.85	3/32	3.59
1	53.8	22.00	535.0	43.15	3/32	3.59
1	63.5	25.45	535.0	51.50	3/32	3.59
1	72.0	28.10	535.0	58.50	3/32	3.59
2	24.5	9.00	536.0	20.10	1/8	6.45
2	36.5	11.80	536.0	30.40	1/8	6.45
2	47.7	14.50	535.0	40.70	1/8	6.45
2	59.5	17.10	535.0	50.50	1/8	6.45
2	70.0	19.70	535.0	60.50	1/8	6.45
3	26.5	12.35	530.5	20.10	3/16	14.79
3	38.5	16.35	529.5	30.40	3/16	14.79
3	50.7	20.25	530.5	40.70	3/16	14.79
3	63.0	24.10	530.5	50.50	3/16	14.79
3	74.0	27.80	532.5	60.50	3/16	14.79
4	24.5	7.85	534.0	20.10	1/4	26.57
4	35.5	10.15	534.0	30.40	1/4	26.57
4	46.6	12.60	534.5	40.70	1/4	26.57
4	58.0	15.00	534.5	50.50	1/4	26.57
4	70.0	17.20	534.5	60.50	1/4	26.57

TABLE III

CALCULATED DATA

AIR ORIFICE CALIBRATION USING CRITICAL FLOW PROVER

1	2	3	4
Air Orifice No.	Q_c* -Air Rate M Ft^3/Day	Q_o** -Air Rate Ft^3/Sec	K - Air Orifice Coefficient
1	5.36	.0619	.0610
1	6.56	.0757	.0603
1	8.77	.101	.0609
1	10.1	.116	.0609
1	11.2	.129	.0609
2	9.37	.109	.135
2	12.2	.141	.134
2	15.1	.174	.135
2	17.8	.206	.134
2	20.55	.237	.135
3	21.6	.249	.257
3	28.3	.327	.257
3	34.8	.402	.257
3	41.2	.475	.255
3	47.4	.547	.258
4	38.6	.447	.604
4	50.5	.583	.605
4	62.3	.720	.605
4	73.5	.848	.598
4	85.0	.980	.598

* $Q_c = \frac{CP}{\sqrt{GT}}$

** $Q_o = K\sqrt{\frac{h_m P_f}{T_f}}$

TABLE IV

CALIBRATION OF BROOKS ROTAMETER

(No.4 Tantalum Spherical Float)

All Runs at Atms. Pressure
Barometer 27.6" Hg.

1	2	3	4	5	6	7
Test No.	Rot. Rdg.	Temp. °F.	Volume Air Ft^3	Time Sec.	Air Rate Ft^3/Sec	Air Rate at 60°F. 14.4 p.s.i. Ft^3/Sec
1	10	73.5	.0300	78.7	.000376	.000345
2	20	73.5	.0500	61.4	.000814	.000747
3	30	73.5	.100	85.5	.00117	.00107
4	40	73.5	.100	64.9	.00154	.00141
5	50	73.5	.100	52.3	.00191	.00175
6	60	73.5	.100	42.2	.00237	.00208
7	70	73.5	.100	36.3	.00275	.00252
8	80	73.5	.200	64.0	.00364	.00334
9	90	73.5	.200	55.0	.00364	.00334
10	100	73.5	.200	49.0	.00408	.00375
11	110	73.5	.200	44.2	.00452	.00415
12	120	73.5	.200	39.7	.00503	.00462
13	130	73.5	.200	36.2	.00552	.00507
14	140	73.5	.200	34.0	.00589	.00541

APPENDIX B

EXPERIMENTAL DATA

TABLE V

SUPPLEMENTARY DATA

Transparent Butyrate Tube

Length of Test Section --	22.88 Ft.	± .02 Ft.
Inside Diameter of Tube -- Nominal 1-inch	1.049 In.	± .005 In.

TABLE VI

EXPERIMENTAL DATA

WATER FLOW DATA

Series A

1	2	3	4	5
Test No.	Water Temp. °F.	Water* Rate ft^3/sec	Pressure Drop Manometer Difference cm. of CCl_4 under H_2O	Air Temp °F.
1	73.0	.00305	2.15	74.5
2	75.5	.00316	2.15	77.0
3	73.0	.00382	3.25	74.5
4	75.5	.00389	3.20	77.0
5	73.0	.00447	4.30	74.5
6	75.5	.00455	4.10	77.0
7	73.0	.00500	5.15	74.5
8	75.5	.00503	5.10	77.0
9	73.0	.00550	6.05	74.5
10	75.5	.00560	6.15	77.0
11	73.0	.00593	6.85	74.5
12	72.5	.00640	7.70	74.5
13	72.5	.00675	8.45	74.5
14	72.0	.00710	9.30	74.5
15	71.5	.00755	10.20	74.5
16	71.5	.00785	10.95	74.5
17	71.5	.00820	11.70	74.5
18	71.5	.00850	12.50	74.5
19	71.5	.00880	13.30	75.0
20	71.5	.00920	13.90	75.0
21	71.5	.00950	14.80	75.0
22	71.5	.00965	15.55	75.0

---

[*] Water flow measured using manometer attached to calibrated orifice.

TABLE VII

EXPERIMENTAL DATA

WATER FLOW DATA

Series B

1	2	3	4	5
Test No.	Water Temp. °F.	Water* Rate ft^3/sec	Pressure Drop Manometer Difference cm. of CCl_4 under H_2O	Air Temp °F.
1	73.0	.00670	8.80	76.5
2	74.0	.00860	13.50	76.0
3	74.5	.00965	16.25	76.5
4	74.5	.0107	19.45	76.5
5	74.5	.0117	22.95	76.5
6	74.5	.0128	27.05	76.5
7	75.0	.0140	31.30	76.5
8	75.0	.0148	34.80	76.5
9	75.0	.0155	37.60	76.5
10	74.5	.0162	40.70	76.5
11	74.5	.0168	43.65	76.5
12	71.5	.0174	46.15	75.0
13	73.5	.0177	48.00	75.0
14	73.5	.0184	51.40	75.5
15	73.5	.0189	53.95	75.0
16	73.5	.0195	56.80	75.0
17	73.5	.0203	60.90	74.5
18	73.5	.0212	65.65	74.5
19	73.5	.0221	71.10	74.5
20	73.5	.0228	75.00	74.5
21	73.5	.0234	78.40	74.5
22	73.5	.0243	83.75	74.5
23	73.5	.0252	89.70	74.5

* Water rate measured using a manometer connected to calibrated orifice.

TABLE VIII

EXPERIMENTAL DATA

WATER FLOW DATA

Series C

1	2	3	4	5
Test No.	Water Temp. °F.	Water* Rate ft^3/sec	Pressure Drop Manometer Difference cm. of Mercury under H_2O	Air Temp °F.
1	73.5	.0165	2.00	77.0
2	73.5	.0200	2.80	77.0
3	73.5	.0233	3.60	77.0
4	73.5	.0260	4.40	77.0
5	73.5	.0285	5.00	77.0
6	73.5	.0308	6.00	77.0
7	73.5	.0325	6.50	77.0
8	73.5	.0340	7.05	77.0
9	73.5	.0367	8.20	77.0
10	73.5	.0384	8.70	77.0
11	73.5	.0402	9.55	77.0
12	73.5	.0420	10.20	77.0
13	74.0	.0445	11.40	77.0
14	74.0	.0460	12.10	77.0
15	73.5	.0480	13.10	77.0
16	74.0	.0492	13.70	77.0
17	73.5	.0505	14.35	77.0
18	74.0	.0520	14.90	77.0
19	73.5	.0532	15.70	77.0
20	73.5	.0555	17.20	77.0
21	74.0	.0569	17.70	77.0
22	73.5	.0582	18.60	77.0

* Water Rate calibrated using manometer attached to calibrated orifice.

TABLE IX

EXPERIMENTAL DATA

Series 1

Constant Water Rate--
4.15 lbs/sec.ft^2

1	2	3	4	5	6	7	8
Test No.	Air Temp. $^\circ$F.	Total Air Rate* ft^3/sec	Water Rate** ft^3/sec	Average Pressure p.s.i.a.	Measured Pressure Drop cm of Hg under air	Vol. Air Between Plug Valves c.c.	Vol. H_2O Between Plug Valves c.c.
1	65.0	.0252	.000400	16.0	6.50	4034	1305
2	65.0	.0478	.000400	16.2	6.50	4170	1169
3	65.0	.0577	.000400	16.0	7.00	4180	1159
4	65.0	.0651	.000400	16.2	8.60	4277	1062
5	65.0	.0716	.000400	16.0	7.90	4212	1127
6	65.0	.0740	.000400	16.0	8.25	4327	1012
7	65.0	.0847	.000400	16.0	8.50	4216	1123
8	65.0	.0852	.000400	16.2	8.50	4294	1045
9	65.0	.101	.000400	16.2	7.80	4341	998
10	75.0	.126	.000400	16.4	7.10	4498	841
11	65.0	.132	.000400	16.2	6.70	4519	820
12	65.0	.152	.000400	16.2	6.80	4570	769
13	75.5	.161	.000400	16.4	6.00	4683	656
14	65.0	.175	.000400	16.3	5.50	4601	738
15	75.0	.209	.000400	16.2	4.65	4777	562
16	75.5	.215	.000400	16.2	4.35	4852	487
17	75.5	.251	.000400	16.2	3.95	4901	438
18	76.0	.293	.000400	16.2	3.70	4952	387
19	75.0	.324	.000400	16.7	3.75	5030	309
20	75.0	.409	.000400	17.1	3.75	5087	252
21	75.0	.510	.000400	17.7	4.45	5137	202
22	75.0	.598	.000400	18.5	4.95	5163	173
23	75.0	.722	.000400	19.3	5.60	5190	149
24	75.0	.812	.000400	20.1	6.30	5196	143
25	70.0	.0113	.000400	16.0	12.70		
26	70.0	.0163	.000400	16.0	9.90		
27	70.0	.0180	.000400	16.0	8.60		
28	70.0	.0223	.000400	16.0	7.70		

* Main air flow measured by manometer connected to air orifice. Air purge measured by rotameter.

** Water flow measured by manometer connected to water orifice.

TABLE X

EXPERIMENTAL DATA

Series 2

Constant Water Rate-- 5.70 lbs/sec.ft^2

1	2	3	4	5	6	7	8
Test No.	Air Temp. °F.	Total Air Rate* ft^3/sec	Water Rate** ft^3/sec	Average Pressure p.s.i.a.	Measured Pressure Drop cm of Hg under air	Vol. Air Between Plug Valves c.c.	Vol. H_2O Between Plug Valves c.c.
1	76.0	.0405	.000550	16.0	6.60	4170	1169
2	76.0	.0491	.000550	16.0	7.10	4127	1212
3	74.0	.0561	.000550	16.2	8.00	4156	1183
4	74.0	.0640	.000550	16.0	7.80	4256	1083
5	76.0	.0707	.000550	16.0	8.40	4198	1141
6	74.0	.0813	.000550	16.2	8.70	4283	1056
7	76.0	.0832	.000550	16.2	9.40	4183	1156
8	74.0	.0832	.000550	16.2	8.60	4166	1173
9	74.0	.0835	.000550	16.2	8.80	4177	1162
10	74.0	.0941	.000550	16.4	8.40	4266	1073
11	74.0	.0987	.000550	16.2	8.40	4363	973
12	74.0	.124	.000550	16.2	8.00	4370	969
13	74.0	.130	.000550	16.2	7.40	4323	1016
14	74.0	.144	.000550	16.2	7.40	4408	931
15	74.0	.152	.000550	16.2	6.80	4505	834
16	74.0	.152	.000550	16.2	6.80	4490	849
17	74.0	.172	.000550	16.2	6.40	4612	727
18	74.0	.204	.000550	16.2	5.40	4745	594
19	74.0	.211	.000550	16.2	4.85	4808	531
20	73.0	.242	.000550	16.3	4.70	4866	473
21	73.0	.277	.000550	16.5	4.25	4934	405
22	74.0	.303	.000550	16.5	4.30	4974	365
23	74.0	.416	.000550	17.3	4.30	5070	269
24	74.0	.486	.000550	17.7	4.80	5112	222
25	74.0	.586	.000550	18.5	5.35	5134	205
26	74.0	.734	.000550	19.7	6.20	5177	162
27	74.0	.946	.000550	21.8	7.80	5198	141
28	70.0	.0133	.000550	16.0	13.90		
29	70.0	.0179	.000550	16.0	8.90		
30	70.0	.0203	.000550	16.0	8.35		
31	70.0	.0229	.000550	16.0	7.50		
32	70.0	.0274	.000550	16.0	6.90		

---

*Main air flow measured by manometer connected to air orifice. Air purge measured by rotameter.

** Water flow measured by manometer connected to orifice.

TABLE XI

EXPERIMENTAL DATA

Series 3

Constant Water Rate--
8.10 lbs/sec.ft^2

1	2	3	4	5	6	7	8
Test No.	Air Temp. °F.	Total Air Rate* ft^3/sec	Water Rate** ft^3/sec	Average Pressure p.s.i.a.	Measured Pressure Drop cm of Hg under air	Vol. Air Between Plug Valves c.c.	Vol. H_2O Between Plug Valves c.c.
1	74.0	.0458	.000780	16.2	7.60		
2	73.0	.0481	.000780	16.1	7.40	4112	1227
3	73.0	.0518	.000780	16.2	7.80	4167	1172
4	74.0	.0685	.000780	16.5	9.00	4219	1120
5	73.0	.0714	.000780	16.0	8.50	4283	1056
6	74.0	.0820	.000780	16.5	9.40	4241	1098
7	75.0	.0994	.000780	16.5	9.30	4156	1183
8	73.0	.121	.000780	16.5	8.60	4348	991
9	74.0	.128	.000780	16.3	8.40	4448	891
10	74.0	.153	.000780	16.3	7.40	4483	856
11	73.0	.173	.000780	16.5	6.80	4634	705
12	75.0	.210	.000780	16.5	5.70	4741	598
13	73.0	.248	.000780	16.7	5.80	4805	534
14	75.0	.276	.000780	17.0	5.40	4870	469
15	74.0	.302	.000780	16.8	5.10	4905	434
16	75.0	.392	.000780	17.5	5.20	5023	316
17	75.0	.474	.000780	18.5	6.00		
18	75.0	.531	.000780	18.7	6.20	5101	238
19	75.0	.598	.000780	19.2	6.60	5123	216
20	75.0	.657	.000780	19.7	7.10	5130	209
21	75.0	.840	.000780	22.0	9.00	5148	191
22	75.0	1.09	.000780	24.5	10.70	5176	163
23	70.0	.0166	.000780	16.0	14.25		
24	70.0	.0200	.000780	16.0	8.90		
25	70.0	.0231	.000780	16.0	8.50		
26	70.0	.0264	.000780	16.0	7.60		
27	70.0	.0283	.000780	16.0	7.50		

* Main air flow measured by manometer connected to air orifice. Air purge measured by rotameter.

** Water flow measured by manometer connected to water orifice.

TABLE XII

EXPERIMENTAL DATA

Series 4

Constant Water Rate--
12.46 lbs/sec.ft^2

1	2	3	4	5	6	7	8
Test No.	Air Temp. °F.	Total Air Rate* ft^3/sec	Water Rate** ft^3/sec	Average Pressure p. s. i. a.	Measured Pressure Drop cm of Hg under air	Vol. Air Between Plug Valves c. c.	Vol. H_2O Between Plug Valves c.c.
1	73.0	.0471	.00120	16.2	8.00	4101	1238
2	73.0	.0610	.00120	16.2	8.70	4134	1205
3	82.0	.0654	.00120	16.5	9.50	4048	1291
4	73.0	.0815	.00120	16.6	9.70	4198	1141
5	74.0	.103	.00120	16.8	9.20	4233	1106
6	85.0	.116	.00120	16.7	9.50	4227	1112
7	70.0	.116	.00120	16.6	10.00	4263	1076
8	72.0	.121	.00120	16.5	9.50	4298	1041
9	73.0	.130	.00120	16.7	9.40	4405	934
10	72.0	.160	.00120	17.0	8.10		
11	74.0	.204	.00120	17.0	6.60	4666	673
12	74.0	.261	.00120	17.2	6.60	4745	594
13	74.5	.290	.00120	17.3	6.55	4798	541
14	75.5	.299	.00120	17.4	6.55	4812	527
15	77.0	.404	.00120	18.5	7.20	4958	381
16	76.0	.474	.00120	19.2	8.80	4970	369
17	77.0	.570	.00120	20.5	8.65	5045	294
18	77.5	.824	.00120	23.5	11.00	5111	228
19	77.5	1.02	.00120	27.0	12.60	5149	190
20	77.5	1.09	.00120	28.0	12.90	5163	176
21	81.0	1.13	.00120	28.0	14.10	5141	198
22	76.0	1.37	.00120	31.0	15.40	5183	156
23	70.0	.0115	.00120	16.1	14.80		
24	70.0	.0175	.00120	16.1	10.20		
25	70.0	.0225	.00120	16.1	8.70		
26	70.0	.0254	.00120	16.1	8.50		
27	70.0	.0294	.00120	16.1	7.75		

---

* Main Air flow measured by manometer connected to water orifice. Air purge measured by rotameter.

** Water flow measured by manometer connected to air orifice.

TABLE XIII
EXPERIMENTAL DATA

Series 5

Constant Water Rate--
17.75 lbs/sec.ft^2

1	2	3	4	5	6	7	8
Test No.	Air Temp. °F.	Total Air Rate* ft^3/sec	Water Rate** ft^3/sec	Average Pressure P.s.i.a.	Measured Pressure Drop cm of Hg under air	Vol. Air Between Plug Valves c.c.	Vol. H_2O Between Plug Valves c.c.
1	71.5	.0306	.00171	16.1	9.00	4019	1320
2	71.5	.0428	.00171	16.3	8.60	4141	1198
3	71.5	.0512	.00171	16.2	9.10	4077	1262
4	73.0	.0547	.00171	16.2	9.50	4083	1256
5	71.5	.0635	.00171	16.2	9.30	4156	1183
6	71.5	.0685	.00171	16.3	9.70	4056	1283
7	72.0	.0720	.00171	16.3	9.80	4145	1193
8	73.5	.0727	.00171	16.2	10.40	4098	1241
9	73.5	.0749	.00171	16.7	10.80	4180	1159
10	76.0	.0903	.00171	16.8	10.70	4274	1065
11	73.5	.0956	.00171	16.7	10.80	4183	1156
12	73.5	.115	.00171	16.8	10.60	4212	1127
13	73.5	.126	.00171	16.8	10.20	4216	1123
14	73.5	.136	.00171	16.8	10.00	4205	1134
15	73.5	.141	.00171	16.8	9.60	4352	983
16	76.0	.143	.00171	16.8	9.50	4441	898
17	73.5	.163	.00171	16.8	9.00	4483	856
18	77.0	.173	.00171	17.2	8.40	4456	883
19	77.0	.213	.00171	17.2	8.10	4590	749
20	77.0	.238	.00171	17.2	7.80	4659	680
21	77.0	.261	.00171	17.3	7.70	4698	641
22	77.0	.296	.00171	17.5	7.70	4763	573
23	77.0	.389	.00171	18.7	8.20	4883	456
24	77.0	.529	.00171	20.5	9.20	4998	342
25	77.0	.625	.00171	21.8	10.20	5027	312
26	77.0	.727	.00171	22.9	11.00	5063	276
27	77.0	.848	.00171	24.6	12.20	5090	249
28	77.0	.941	.00171	26.2	13.10	5112	227
29	77.0	1.06	.00171	27.5	13.80	5123	216
30	77.0	1.15	.00171	28.4	14.55	5132	207
31	78.0	1.28	.00171	30.0	15.40	5152	187
32	78.0	1.44	.00171	34.0	16.30	5166	173
33	70.0	.0113	.00171	16.1	16.30		
34	70.0	.0185	.00171	16.1	11.55		
35	70.0	.0235	.00171	16.1	9.80		
36	70.0	.0268	.00171	16.1	9.10		
37	70.0	.0297	.00171	16.1	9.10		

---

* Main air flow measured by manometer connected to water orifice. Air purge measured by rotameter.

** Water flow measured by manometer connected to air orifice.

TABLE XIV
EXPERIMENTAL DATA

Series 6

Constant Water Rate--
25.1 lbs/sec.ft^2

1	2	3	4	5	6	7	8
Test No.	Air Temp. °F.	Total Air Rate* ft^3/sec	Water Rate** ft^3/sec	Average Pressure p.s.i.a.	Measured Pressure Drop cm of Hg under air	Vol. Air Between Plug Valves c.c.	Vol. H_2O Between Plug Valves c.c.
1	75.0	.0269	.00242	17.0	10.80	3756	1583
2	76.0	.0380	.00242	16.7	10.00	3956	1383
3	76.0	.0429	.00242	16.5	9.80	4041	1298
4	76.0	.0489	.00242	16.5	9.80	4056	1283
5	76.0	.0557	.00242	16.6	10.00	4083	1256
6	76.0	.0643	.00242	16.5	10.20	4059	1280
7	76.0	.0674	.00242	16.7	10.40	4027	1312
8	75.0	.0691	.00242	16.9	10.80	4134	1205
9	73.0	.0753	.00242	16.8	10.70	4108	1231
10	73.0	.0828	.00242	16.8	11.00	4083	1256
11	73.0	.0834	.00242	17.1	11.20	4063	1276
12	78.0	.0955	.00242	17.0	11.70	4108	1231
13	75.0	.103	.00242	17.0	11.40	4070	1269
14	75.0	.118	.00242	17.0	11.50	4141	1198
15	75.0	.133	.00242	17.1	11.00	4277	1062
16	75.0	.159	.00242	17.2	10.60	4212	1127
17	78.0	.161	.00242	17.0	10.40	4534	805
18	78.0	.178	.00242	17.3	10.00	4241	1098
19	78.0	.202	.00242	17.0	9.60	4687	652
20	78.0	.242	.00242	17.2	9.65	4519	820
21	78.0	.269	.00242	18.0	9.65	4598	740
22	70.0	.291	.00242	18.5	9.30	4641	698
23	78.0	.326	.00242	18.5	9.80	4677	662
24	70.0	.337	.00242	19.2	10.80		
25	78.0	.363	.00242	19.2	10.05	4741	598
26	70.0	.435	.00242	19.3	10.90		
27	70.0	.557	.00242	22.0	11.65	4941	398
28	70.0	.642	.00242	23.5	12.10		
29	70.0	.702	.00242	24.5	13.40		
30	70.0	.768	.00242	25.3	14.20		
31	70.0	.851	.00242	27.0	14.90		
32	70.0	.934	.00242	27.8	15.40	5056	283
33	70.0	.986	.00242	28.5	15.95		
34	70.0	1.07	.00242	29.8	16.50		
35	70.0	1.15	.00242	30.2	16.90	5083	256
36	70.0	1.40	.00242	33.0	18.80		
37	70.0	.0116	.00242	16.1	17.90		
38	70.0	.0192	.00242	16.1	13.00		
39	70.0	.0252	.00242	16.1	10.80		
40	70.0	.0301	.00242	16.1	10.00		

---

* Main air flow measured by manometer connected to water orifice. Air purge measured by rotameter.

** Water flow measured by manometer connected to air orifice.

TABLE XV

EXPERIMENTAL DATA

Series 7

Constant Water Rate--
51.8 lbs/sec.ft^2

1	2	3	4	5	6	7	8
Test No.	Air Temp. °F.	Total Air Rate* ft^3/sec	Water Rate** ft^3/sec	Average Pressure p.s.i.a.	Measured Pressure Drop cm of Hg under air	Vol. Air Between Plug Valves c.c.	Vol. H_2O Between Plug Valves c.c.
1	76.5	.0424	.00500	17.5	12.50	3614	1725
2	74.0	.0457	.00500	17.5	13.10		
3	76.5	.0499	.00500	17.7	12.40	3787	1552
4	75.0	.0524	.00500	18.5	13.40		
5	76.5	.0582	.00500	18.0	13.40	3870	1469
6	76.5	.0741	.00500	18.0	13.10	4033	1306
7	73.0	.0770	.00500	18.0	13.10	3933	1406
8	75.5	.117	.00500	19.0	12.50	4033	1306
9	74.5	.128	.00500	19.0	13.70	4212	1127
10	74.5	.164	.00500	19.5	13.00	4183	1156
11	75.0	.171	.00500	19.5	13.60		
12	74.5	.192	.00500	19.5	13.70	4174	1165
13	75.0	.274	.00500	20.5	12.90	4456	883
14	74.5	.320	.00500	21.5	14.00	4483	856
15	75.5	.342	.00500	33.0	14.20	4390	949
16	75.5	.369	.00500	22.5	14.10	4527	812
17	75.5	.432	.00500	23.5	15.30	4612	727
18	76.0	.461	.00500	24.0	15.30	4627	712
19	75.0	.527	.00500	25.7	16.65	4683	656
20	74.5	.567	.00500	33.0	16.60	4656	683
21	74.5	.627	.00500	28.0	18.50	4694	645
22	74.5	.779	.00500	31.0	20.60	4812	527
23	74.5	.839	.00500	32.0	21.15	4805	534
24	74.5	.866	.00500	32.3	21.25	4812	527
25	74.5	.871	.00500	32.5	21.10	4819	520
26	74.5	.894	.00500	33.0	21.15	4827	512

---

* Main air flow measured by manometer connected to water orifice. Air purge measured by rotameter.

** Water flow measured by manometer connected to air orifice.

APPENDIX C

CALCULATED RESULTS

TABLE XVI

CALCULATED DATA

WATER FLOW RESULTS

Series A

1	2	3	4	5
Test No.	Pressure Drop-F ft. of H_2O	Velocity- V ft./sec.	Reynolds Number *	Friction Factor **
1	.0415	.508	4240	.00988
2	.0416	.526	4370	.00922
3	.0627	.636	5300	.00952
4	.0618	.648	5420	.00903
5	.0830	.745	6320	.00919
6	.0792	.757	6320	.00847
7	.106	.833	6950	.00935
8	.0965	.838	7000	.00842
9	.117	.916	7650	.00855
10	.116	.934	7800	.00817
11	.132	.988	8250	.00840
12	.149	1.07	8900	.00800
13	.163	1.13	9400	.00788
14	.180	1.18	9900	.00788
15	.197	1.26	10500	.00765
16	.211	1.31	10900	.00757
17	.226	1.37	11400	.00746
18	.241	1.42	11800	.00740
19	.257	1.47	12200	.00733
20	.268	1.53	12800	.00731
21	.286	1.58	13200	.00703
22	.300	1.61	13400	.00713

* $\frac{D V \rho}{\mu}$

** $\frac{F \rho D}{V^2 \; 2N_c}$

TABLE XVII

CALCULATED DATA

WATER FLOW RESULTS

Series B

1 Test No.	2 Pressure Drop-F ft. of H_2O	3 Velocity- V ft./sec.	4 Reynolds Number *	5 Friction Factor **
1	.170	1.12	9300	.00835
2	.255	1.44	12000	.00760
3	.312	1.61	13400	.00742
4	.375	1.79	14800	.00725
5	.432	1.95	16300	.00698
6	.521	2.14	17800	.00703
7	.603	2.33	19500	.00679
8	.671	2.47	20600	.00676
9	.725	2.59	21600	.00668
10	.785	2.70	22500	.00660
11	.842	2.80	23400	.00658
12	.872	2.90	24200	.00636
13	.926	2.95	24700	.00653
14	.992	3.07	25700	.00646
15	1.04	3.15	26300	.00643
16	1.10	3.25	27200	.00634
17	1.18	3.39	28300	.00627
18	1.27	3.54	29600	.00621
19	1.37	3.69	30800	.00618
20	1.45	3.80	31700	.00612
21	1.51	3.90	32600	.00610
22	1.62	4.06	33900	.00602
23	1.73	4.20	35100	.00600

* $\dfrac{D\,V\,\rho}{\mu}$

** $\dfrac{F\,g\,D}{V^2\;2N_c}$

TABLE XVIII

CALCULATED DATA

WATER FLOW RESULTS

Series C

1	2	3	4	5
Test No.	Pressure Drop-F ft. of H_2O	Velocity- V ft./sec.	Reynolds Number *	Friction Factor **
1	.826	2.75	23000	.00672
2	1.16	3.34	27900	.00634
3	1.49	3.88	32400	.00606
4	1.82	4.33	36200	.00594
5	2.07	4.75	39600	.00566
6	2.48	5.14	42900	.00577
7	2.69	5.42	45300	.00562
8	2.91	5.67	47300	.00556
9	3.38	6.14	51200	.00548
10	3.60	6.40	53400	.00539
11	3.94	6.71	56000	.00537
12	4.22	7.00	58400	.00528
13	4.72	7.42	62000	.00523
14	5.01	7.67	64100	.00523
15	5.41	8.00	66800	.00519
16	5.67	8.21	68600	.00516
17	5.94	8.42	70300	.00514
18	6.16	8.67	72300	.00505
19	6.49	8.87	74100	.00507
20	7.11	9.25	77200	.00508
21	7.32	9.49	79200	.00500
22	7.68	9.70	81800	.00502

* $\frac{D V e}{\mu}$

** $\frac{F \beta D}{V^2 \; 2N_e}$

TABLE XIX

CALCULATED DATA

Series 1 — Constant Water Rate-- 4.15 lbs/sec.ft^2

1	2	3	4	5	6	7	8	9
Test No.	Disch. Air-H_2O Ratio ft^3 s.c. /ft^3	Test Sect. Air-H_2O Ratio ft3/ft^3	Air Rate-G lbs/sec	Water Rate-L lbs/sec	Spec.* Vol. Air-v_G ft^3/lbs	Dis.** Hydro-static Head p.s.i. /100ft.	Meas. Pressure Drop p.s.i. /100ft.	Meas. Pressure Drop Minus Total Head H_2O in Tube p.s.i./100ft.
1	63.0	3.08	.00188	.0249	12.5	.776	5.50	-5.11
2	122	3.57	.00358	.0249	12.3	.444	5.50	-3.21
3	144	3.62	.00432	.0249	12.5	.374	5.92	-3.50
4	162	4.01	.00487	.0249	12.3	.342	7.25	-1.40
5	179	3.75	.00536	.0249	12.5	.324	6.67	-2.49
6	185	4.28	.00552	.0249	12.5	.395	6.96	-1.22
7	211	3.77	.00633	.0249	12.5	.271	7.18	-1.94
8	213	4.11	.00637	.0249	12.3	.275	7.18	-1.27
9	253	4.36	.00758	.0249	12.3	.241	6.59	-1.52
10	315	5.23	.00940	.0249	12.4	.258	6.00	- .85
11	330	5.50	.00985	.0249	12.3	.201	5.66	-1.02
12	380	5.93	.0114	.0249	12.3	.178	5.74	- .53
13	402	7.12	.0120	.0249	12.4	.172	5.07	- .25
14	438	6.23	.0131	.0249	12.3	.163	4.65	-1.39
15	522	8.50	.0156	.0249	12.6	.143	3.93	- .63
16	537	10.0	.0161	.0249	12.6	.140	3.67	- .30
17	628	11.2	.0188	.0249	12.6	.128	3.34	- .21
18	732	12.8	.0219	.0249	12.6	.107	3.13	.00
19	810	16.3	.0242	.0249	12.2	.114	3.17	.63
20	1020	20.1	.0306	.0249	11.9	.108	3.17	1.10
21	1270	25.4	.0381	.0249	11.5	.103	3.76	2.10
22	1490	29.8	.0447	.0249	11.0	.098	4.18	2.79
23	1800	34.8	.0538	.0249	10.5	.096	4.73	3.51
24	2030	36.3	.0606	.0249	10.0	.096	5.22	4.15
25	28.2		.000845	.0249	12.7	1.63	10.75	
26	40.8		.00122	.0249	12.7	1.15	8.37	
27	45.0		.00134	.0249	12.7	1.06	7.27	
28	55.8		.00167	.0249	12.7	.86	6.50	

---

* At average pressure

** $$\frac{\left(\frac{G}{L}\right)_{av.} + 1}{\left(\frac{G}{L} v_G\right)_{av.} + v_L}$$ (See equation 28)

TABLE XX

CALCULATED DATA

Series 2 Constant Water Rate—5.70 lbs/sec.ft^2

1	2	3	4	5	6	7	8
Test No.	Disch. Air-H_2O Ratio ft^{3}s.c./ft^3	Test Sect. Air-H_2O Ratio ft^3/ft^3	Air Rate-G lbs/sec	Water Rate-L lbs/sec	Spec.* Vol. Air-v_G ft^3/lbs	Dis.** Hydro-static Head psi/100ft	Meas. Pressure Drop psi/100ft
1	73.7	3.58	.00303	.0342	12.8	.658	5.57
2	89.5	3.41	.00367	.0342	12.8	.550	6.00
3	102	3.52	.00420	.0342	12.5	.500	6.76
4	116	3.93	.00479	.0342	12.7	.439	6.59
5	128	3.67	.00530	.0342	12.8	.415	7.10
6	148	4.05	.00608	.0342	12.5	.366	7.35
7	151	3.62	.00623	.0342	12.6	.356	7.94
8	151	3.53	.00623	.0342	12.5	.360	7.27
9	152	3.58	.00625	.0342	12.6	.353	7.44
10	171	3.97	.00705	.0342	12.4	.325	7.10
11	179	4.48	.00738	.0342	12.6	.247	6.25
12	226	4.52	.00925	.0342	12.5	.260	6.75
13	236	4.25	.00973	.0342	12.6	.247	6.25
14	262	4.73	.0108	.0342	12.5	.231	6.25
15	277	5.42	.0114	.0342	12.5	.222	5.74
16	277	5.28	.0114	.0342	12.6	.220	5.75
17	313	6.35	.0129	.0342	12.6	.200	5.41
18	371	7.98	.0152	.0342	12.6	.178	4.57
19	384	9.05	.0158	.0342	12.6	.174	4.10
20	440	10.3	.0181	.0342	12.5	.160	3.98
21	505	12.2	.0207	.0342	12.3	.150	3.59
22	552	13.6	.0227	.0342	12.3	.141	3.63
23	757	18.8	.0311	.0342	11.7	.124	3.63
24	885	23.0	.0363	.0342	11.5	.116	4.06
25	1060	25.0	.0438	.0342	11.0	.112	4.52
26	1330	31.9	.0548	.0342	10.3	.109	5.24
27	1720	36.9	.0708	.0342	9.3	.110	6.58
28	20.5		.000845	.0342	12.7	2.17	11.75
29	32.6		.00134	.0342	12.7	1.41	7.52
30	37.0		.00152	.0342	12.7	1.25	7.05
31	41.7		.00171	.0342	12.7	1.12	6.34
32	50.2		.00205	.0342	12.7	.950	5.83

---

* At average pressure

**

$$\frac{(\frac{G}{L})_{av.} + 1}{(\frac{G}{L} v_G)_{av.} + v_L}$$

(See equation 28)

TABLE XXI

CALCULATED DATA

Series 3

Constant Water Rate--
8.10 lbs/sec.ft^3

1	2	3	4	5	6	7	8
Test No.	Disch. Air-H_2O Ratio ft^{3}s.c. /ft^3	Test Sect. Air-H_2O Ratio ft^3/ft^3	Air Rate-G lbs/sec	Water Rate-L lbs/sec	Spec.* Vol. Air-v_G ft^3/lbs	Dis.** Hydro-static Head psi/100ft	Meas. Pressure Drop psi/100ft
1	58.7		.00342	.0486	12.5	.835	6.42
2	61.6	3.36	.00360	.0486	12.6	.785	6.25
3	66.4	3.55	.00398	.0486	12.5	.723	6.59
4	87.8	3.77	.00517	.0486	12.3	.578	7.61
5	91.5	4.06	.00534	.0486	12.7	.537	7.18
6	105	3.87	.00613	.0486	12.3	.498	7.95
7	127	3.52	.00743	.0486	12.3	.422	7.86
8	155	4.37	.00905	.0486	12.3	.356	7.26
9	164	4.98	.00956	.0486	12.4	.337	7.10
10	196	5.22	.0114	.0486	12.4	.293	6.25
11	221	6.58	.0129	.0486	12.3	.268	5.74
12	269	7.95	.0157	.0486	12.3	.230	4.82
13	308	9.00	.0185	.0486	12.2	.205	4.90
14	353	10.4	.0206	.0486	11.9	.196	4.57
15	387	11.3	.0226	.0486	12.1	.180	4.31
16	502	15.9	.0293	.0486	11.6	.159	4.39
17	609		.0355	.0486	11.0	.149	5.07
18	680	21.4	.0397	.0486	10.8	.142	5.23
19	765	23.7	.0448	.0486	10.5	.137	5.57
20	842	24.5	.0492	.0486	10.3	.134	6.00
21	1080	26.9	.0628	.0486	9.20	.134	7.60
22	1400	31.7	.0814	.0486	8.20	.134	9.05
23	14.8		.000868	.0486	12.7	2.94	12.05
24	25.6		.00150	.0486	12.7	1.83	7.52
25	29.6		.00173	.0486	12.7	1.59	7.18
26	33.8		.00197	.0486	12.7	1.37	6.42
27	36.3		.00212	.0486	12.7	1.27	6.33

* At average pressure

** $$\frac{\left(\frac{G}{L}\right)_{av.} + 1}{\left(\frac{G}{L} v_G\right)_{av.} + v_L}$$ (See equation 28)

TABLE XXII

CALCULATED DATA

Series 4

Constant Water Rate--
12.46 lbs/sec.ft^2

1	2	3	4	5	6	7	8
Test No.	Disch. Air-H_2O Ratio ft^{3}s.c. /ft^3	Test Sect. Air-H_2O Ratio ft^3/ft^3	Air Rate-G lbs/sec	Water Rate-L lbs/sec	Spec.* Vol. Air-v_G ft^3/lbs	Dis.** Hydro-static Head psi/100ft	Meas. Pressure Drop psi/100ft
1	39.2	3.32	.00352	.0748	12.5	1.20	6.75
2	50.8	3.43	.00456	.0748	12.5	.945	7.35
3	54.4	3.14	.00488	.0748	12.5	.890	8.03
4	67.8	3.66	.00610	.0748	12.2	.745	8.20
5	86.1	3.82	.00773	.0748	12.1	.567	7.78
6	96.5	3.80	.00868	.0748	12.3	.530	8.03
7	96.8	3.98	.00869	.0748	12.2	.543	8.45
8	101	4.11	.00905	.0748	12.3	.515	8.03
9	108	4.72	.00972	.0748	12.1	.495	7.95
10	133		.0120	.0748	11.9	.422	6.85
11	170	6.34	.0152	.0748	12.0	.341	5.58
12	218	8.00	.0195	.0748	11.8	.283	5.58
13	242	8.83	.0217	.0748	11.8	.260	5.54
14	249	9.15	.0223	.0748	11.7	.250	5.54
15	337	13.0	.0302	.0748	11.0	.219	6.08
16	397	13.5	.0354	.0748	10.6	.203	7.44
17	475	17.1	.0426	.0748	9.90	.192	7.31
18	687	22.4	.0615	.0748	8.63	.178	9.30
19	851	27.1	.0763	.0748	7.50	.183	10.60
20	910	29.3	.0815	.0748	7.23	.166	10.90
21	935	25.9	.0898	.0748	7.18	.176	11.90
22	1140	33.2	.102	.0748	6.55	.184	13.00
23	9.60		.000845	.0748	12.6	4.37	12.50
24	14.6		.00131	.0748	12.6	3.18	8.61
25	18.7		.00168	.0748	12.6	2.49	7.35
26	21.2		.00190	.0748	12.6	2.21	7.18
27	24.5		.00220	.0748	12.6	1.91	6.55

* At average pressure

**

$$\frac{\left(\frac{G}{L}\right)_{av.} + 1}{\left(\frac{G}{L} v_G\right)_{av.} + v_L}$$

(See equation 28)

TABLE XXIII

CALCULATED DATA

Series 5

Constant Water Rate--
17.75 lbs/sec.ft^2

1	2	3	4	5	6	7	8
Test No.	Disch. Air-H_2O Ratio ft^{3}s.c./ft^3	Test Sect. Air-H_2O Ratio ft^3/ft^3	Air Rate-G lbs/sec	Water Rate-L lbs/sec	Spec.* Vol. Air-v_G ft^3/lbs	Dis.** Hydro-static Head psi/100ft	Meas. Pressure Drop psi/100ft
1	17.9	3.05	.00229	.107	12.6	2.47	7.60
2	25.1	3.46	.00320	.107	12.5	1.83	7.25
3	30.0	3.23	.00383	.107	12.5	1.55	7.69
4	32.0	3.25	.00409	.107	12.1	1.50	8.03
5	37.2	3.51	.00475	.107	12.5	1.27	7.85
6	40.1	3.16	.00512	.107	12.4	1.19	8.20
7	42.2	3.47	.00538	.107	12.4	1.14	8.28
8	42.6	3.31	.00544	.107	12.1	1.15	8.80
9	43.8	3.61	.00560	.107	12.1	1.12	9.12
10	52.8	4.02	.00674	.107	12.1	.945	9.05
11	56.0	3.62	.00715	.107	12.1	.897	9.12
12	67.4	3.75	.00860	.107	12.1	.755	8.95
13	73.8	3.76	.00941	.107	12.1	.695	8.62
14	79.6	3.71	.0102	.107	12.1	.645	8.45
15	82.5	4.43	.0105	.107	12.0	.631	8.10
16	83.5	4.95	.0106	.107	12.1	.627	8.02
17	95.5	5.23	.0122	.107	12.0	.565	7.60
18	101	5.05	.0129	.107	11.8	.538	7.10
19	124	6.13	.0159	.107	11.8	.453	6.85
20	139	6.85	.0178	.107	11.8	.406	6.58
21	153	7.32	.0195	.107	11.7	.384	6.50
22	173	8.32	.0221	.107	11.6	.350	6.50
23	227	10.7	.0290	.107	10.8	.299	6.92
24	310	14.6	.0395	.107	9.90	.259	7.72
25	365	16.1	.0467	.107	9.30	.244	8.60
26	425	18.3	.0542	.107	8.80	.234	9.30
27	495	19.6	.0633	.107	8.40	.220	10.3
28	550	22.5	.0703	.107	7.70	.227	11.0
29	620	23.7	.0791	.107	7.35	.223	11.7
30	673	24.8	.0860	.107	7.12	.219	12.3
31	748	27.5	.0955	.107	6.72	.218	13.0
32	842	29.8	.107	.107	6.30	.219	13.8
33	6.60		.000860	.107	12.6	6.02	13.8
34	10.8		.00138	.107	12.6	3.94	9.76
35	13.7		.00176	.107	12.6	3.14	8.28
36	15.7		.00200	.107	12.6	2.80	7.69
37	17.3		.00222	.107	12.6	2.56	7.69

* At average pressure

** $$\frac{(\frac{G}{L})_{av.} + 1}{(\frac{G}{L} v_G)_{av.} + v_L}$$ (See Equation 28)

TABLE XXIV

CALCULATED DATA

Series 6

Constant Water Rate--
25.1 lbs/sec.ft^2

1	2	3	4	5	6	7	8
Test No.	Disch. Air-H_2O Ratio ft^{3}s.c./ft^3	Test Sect. Air-H_2O Ratio ft^3/ft^3	Air Rate-G lbs/sec	Water Rate-L lbs/sec	Spec.* Vol. Air-v_G ft^3/lbs	Dis.** Hydro-static Head psi/100ft	Meas. Pressure Drop psi/100ft
1	11.1	2.37	.00201	.151	12.0	3.99	9.12
2	15.7	2.87	.00284	.151	12.2	3.03	8.45
3	17.7	3.11	.00321	.151	12.4	2.53	8.28
4	20.2	3.16	.00366	.151	12.4	2.23	8.28
5	23.0	3.24	.00417	.151	12.3	2.01	8.45
6	26.6	3.18	.00482	.151	12.4	1.73	8.62
7	27.8	3.06	.00504	.151	12.2	1.70	8.78
8	28.6	3.43	.00517	.151	12.0	1.68	9.12
9	31.1	3.33	.00563	.151	12.1	1.48	9.05
10	34.2	3.23	.00619	.151	12.1	1.42	9.30
11	34.5	3.19	.00623	.151	11.9	1.42	9.45
12	39.5	3.34	.00715	.151	12.0	1.23	9.90
13	42.5	3.21	.00768	.151	11.9	1.18	9.64
14	48.8	3.45	.00882	.151	11.9	1.03	9.72
15	55.0	4.00	.00995	.151	11.9	.932	9.30
16	65.7	3.74	.0119	.151	11.8	.792	8.96
17	66.6	5.63	.0120	.151	12.0	.770	8.80
18	73.5	3.86	.0133	.151	11.8	.723	8.45
19	83.5	7.18	.0151	.151	12.0	.628	8.12
20	100	5.50	.0181	.151	11.9	.536	8.15
21	111	6.20	.0201	.151	11.3	.518	8.15
22	120	6.65	.0217	.151	11.0	.496	7.85
23	135	7.07	.0242	.151	11.0	.454	8.28
24	139		.0252	.151	10.6	.453	9.13
25	150	7.93	.0271	.151	10.6	.431	8.50
26	180		.0325	.151	9.54	.408	9.20
27	225	12.4	.0417	.151	9.02	.356	9.85
28	260		.0480	.151	8.60	.332	10.2
29	287		.0525	.151	8.26	.325	11.3
30	312		.0573	.151	8.00	.315	12.0
31	352		.0636	.151	7.48	.312	12.6
32	386	17.9	.0698	.151	7.26	.305	13.0
33	408		.0737	.151	7.10	.298	13.5
34	442		.0800	.151	6.76	.290	13.9
35	476	19.8	.0860	.151	6.68	.286	14.3
36	580		.105	.151	6.40	.280	15.9
37	4.80		.000868	.151	12.5	8.00	15.1
38	7.90		.00143	.151	12.6	5.19	11.0
39	10.4		.00188	.151	12.6	4.10	9.13
40	12.9		.00225	.151	12.6	3.46	8.45

* At average pressure.

** $$\frac{(\frac{G}{L})_{av.} + 1}{(\frac{G}{L} v_G)_{av.} + v_L}$$ (See equation 28)

TABLE XXV

CALCULATED DATA

Series 7

Constant Water Rate--
51.8 lbs/sec.ft^2

1	2	3	4	5	6	7	8
Test No.	Disch. Air-H_2O Ratio ft^3s.c. /ft^3	Test Sect. Air-H_2O Ratio ft^3/ft^3	Air Rate-G lbs/sec	Water Rate-L lbs/sec	Spec.* Vol. Air-v_G ft^3/lbs	Dis.** Hydro-static Head psi/100ft	Meas. Pres-sure Drop psi/100ft.
1	8.48	2.10	.00315	.311	11.7	5.21	10.6
2	9.14		.00342	.311	11.6	4.88	10.7
3	9.98	2.43	.00373	.311	11.5	4.53	10.5
4	10.3		.00392	.311	11.0	4.57	11.3
5	11.6	2.54	.00453	.311	11.3	3.90	11.3
6	14.8	3.08	.00554	.311	11.3	3.25	11.1
7	15.4	2.80	.00576	.311	11.2	3.18	11.1
8	23.4	3.08	.00873	.311	10.7	2.26	10.6
9	25.6	3.74	.00955	.311	10.6	2.15	11.6
10	32.8	3.61	.0123	.311	10.4	1.70	11.0
11	34.2		.0128	.311	10.4	1.62	11.5
12	38.4	3.58	.0144	.311	10.4	1.46	11.6
13	54.8	5.05	.0208	.311	9.90	1.10	10.9
14	64.0	5.23	.0239	.311	9.40	1.00	11.8
15	68.4	4.63	.0256	.311	6.10	1.48	12.0
16	73.8	5.57	.0276	.311	9.00	.925	11.9
17	86.4	6.34	.0323	.311	8.60	.840	12.9
18	92.2	6.50	.0345	.311	8.40	.813	12.9
19	105	7.13	.0394	.311	7.86	.778	14.1
20	113	6.67	.0417	.311	6.10	.945	14.0
21	125	7.28	.0468	.311	7.20	.730	15.6
22	155	9.12	.0582	.311	6.50	.672	17.3
23	167	9.00	.0627	.311	6.30	.653	17.9
24	173	9.12	.0647	.311	6.25	.638	18.0
25	174	9.30	.0652	.311	6.20	.638	17.8
26	179	9.45	.0668	.311	6.10	.637	17.9

* At average pressure

**

$$\frac{(\frac{G}{L})_{av.} + 1}{(\frac{G}{L} v_G)_{av.} + v_L}$$

(See equation 28)

TABLE XXVI

VARIATION OF HOLDUP WITH AIR-H_2O DISCHARGE RATIO

Values obtained from Figure 13

Constant Water Rate--
4.15 lbs/sec.ft^2

1	2	3
Discharge Air-H_2O Ratio ft^3s.c./ft^3	Test Section Air-H_2O Ratio ft^3/ft^3	Discharge Air-H_2O Ratio / Test Section Air-H_2O Ratio ft^3s.c./ft^3 ft^3/ft^3
60	3.20	18.7
110	3.50	31.2
200	4.00	50.0
315	5.00	63.0
385	6.00	64.3
440	7.00	63.0
485	8.00	60.1
525	9.00	58.3
565	10.00	56.0
605	11.00	55.0
640	12.00	53.3
676	13.00	52.0
720	14.00	51.5
760	15.00	50.7
805	16.00	50.3
855	17.00	50.2
905	18.00	50.2
1005	20.00	50.2
1270	25.00	51.0
1535	30.00	51.2
1785	35.00	51.2

TABLE XXVII

VARIATION OF MAXIMUM AND MINIMUM POINTS WITH H_2O RATES

Values from Figures 15-21

1	2		3		4	
Water Rate	Minimum "Slugging"		Maximum "Froth"		Minimum "Film"	
	Measured Pressure Drop	Discharge Air-H_2O Ratio	Measured Pressure Drop	Discharge Air-H_2O Ratio	Measured Pressure Drop	Discharge Air-H_2O Ratio
lbs/sec ft^2	psi/100ft	ft^{3}s.c./ft^3	psi/100ft	ft^{3}s.c./ft^3	psi/100ft	ft^{3}s.c./ft^3
4.15	5.20	95	7.20	210	3.05	825
5.70	5.50	65	7.30	160	3.50	620
8.10	6.05	50	7.90	115	4.30	425
12.46	6.55	37	8.30	75	5.50	215
17.75	7.30	25	9.15	58	6.50	165
25.1	8.30	20	9.80	50	8.00	120
51.8			11.70	25	11.20	55

TABLE XXVIII

VARIATION OF MAXIMUM AND MINIMUM POINTS WITH WATER RATES

Values from Figures 15-21

1	2		3		4	
Water Rate	Minimum "Slugging"		Maximum "Froth"		Minimum "Film"	
	Air-H_2O Ratio in Test Section	Air Rate	Air-H_2O Ratio in Test Section	Air Rate	Air-H_2O Ratio in Test Section	Air Rate
lbs/secft^2	ft^3/ft^3	ft^3/sec	ft^3/ft^3	ft^3/sec	ft^3/ft^3	ft^3/sec
4.15	3.0	.038	4.0	.084	17.5	.33
5.70	3.2	.036	3.8	.088	16.0	.34
8.10	3.2	.039	3.8	.089	11.5	.33
12.46	3.2	.044	3.8	.090	7.5	.27
17.75	3.0	.043	3.8	.099	7.8	.28
25.1	3.1	.044	3.5	.120	5.5	.29
51.8			3.8	.125	4.5	.28

NOMENCLATURE

C - Critical Flow Constant

D - Diameter of Pipe, Ft.

F - Pressure Drop, Ft. of Flowing Fluid

f - Friction Factor, see Text

G - Air Rate, lbs/sec

g - Local Acceleration of Gravity, Ft./Sec.^{2}

H - Height of Vertical Section, Ft.

h_m - Differential Manometer Reading Inches of Mercury under Air

K - Air Orifice Constant

L - Water Rate, lbs/sec

M - Molecular Weight

m - Mass, Lbs.

N_e - Equivalent Length of Section, Ft.

P - Pressure, lbs/ft^2

P_b - Pressure at Bottom of Section, lbs/ft^2

ΔP_f - "Pressure Drop" due to Frictional Effects, lbs/ft^2

P_f - Upstream Air Pressure, P.S.I.A.

ΔP_{LH} - "Pressure Drop" due to Hydrostatic Head of Liquid, lbs/ft^2

P_r - Pressure in Rotameter, P.S.I.A.

P_t - Pressure at Top of Section, lbs/ft^2

Q_c - Rate of Gas Flow, 1000ft^3/24hrs at 14.4 P.S.I.A. and 60°F.

Q_o - Air Rate, ft^3/sec. at 14.4 P.S.I.A. and 60°F.

q - Heat Transfer of Energy

R - Gas Constant

R_e - Reynolds number, see Text

T - Absolute Temperature

NOMENCLATURE (CONT'D)

T_f - Air Orifice Temperature, $^{\circ}$A.

T_r - Rotameter Temperature, $^{\circ}$A.

ΔU - All Energy of System Exclusive of Potential and Kinetic Energy.

V - Velocity, ft/sec

v - Specific Volume

v_G - Specific Volume of air

v_L - Specific Volume of Water

w - All Other Forms of Energy Transferred

w_f - Friction

w_s - Shaft Work

X - Position Above Datum, ft.

y - Volume Fraction of Pipe Occupied by Liquid

β - Constant of Proportionality $\frac{\text{mass lbs}}{\text{force lbs}} \quad \frac{\text{ft}}{\text{sec}^2}$

γ - Surface Tension, lbs.force/ft.

μ - Viscosity, lbs/sec.ft.

ρ - Density, lbs/ft^3

σ - Surface Area of System, Ft^2

Note: See Text for explanation of nomenclature not included in this list.

BIBLIOGRAPHY

1. Cromer, S. and Huntington, R.L.--Visual Studies of the Flow of Air-Water Mixtures in a Vertical Pipe--Trans. A.I.M.E., 136:79, 1940.
2. Dodge, B.F.--Chemical Engineering Thermodynamics--McGraw-Hill Book Company, New York, 1944.
3. Gosiline, J.E.--Experiments on the Vertical Flow of Gas-Liquid Mixtures through Vertical Pipes--Trans. A.I.M.E., 118:56, 1936.
4. Moore, T.V. and Wilde, H.D., Jr.--Experimental Measurement of Slippage in Flow Through Vertical Pipes--Trans. A.I.M.E., 92:296, 1931.
5. Rouse, H.--Elementary Mechanics of Fluids--Wiley, 1946.
6. Uren, L.C. et al.--Flow Resistance of Gas-Oil Mixtures through Vertical Pipes--Trans. A.I.M.E., 86:209, 1930.
7. Versuluys, J.--Some Principles Governing the Choice of Length and Diameter of Tubing in Oil Wells--Trans. A.I.M.E., 92:293, 1931.

B29759 12